NASA Technical Paper 1270

Estimation of Leading-Edge Thrust for Supersonic Wings of Arbitrary Planform

Harry W. Carlson and Robert J. Mack

OCTOBER 1978

NASA

NASA Technical Paper 1270

Estimation of Leading-Edge Thrust for Supersonic Wings of Arbitrary Planform

Harry W. Carlson and Robert J. Mack
Langley Research Center
Hampton, Virginia

National Aeronautics
and Space Administration

**Scientific and Technical
Information Office**

1978

SUMMARY

A numerical method for the estimation of leading-edge thrust for supersonic wings of arbitrary planform has been developed and has been programmed as an extension to an existing high-speed digital computer method for prediction of wing pressure distributions. The accuracy of the method is assessed by comparison with linearized-theory results for a series of flat delta wings. Application of the method to wings of arbitrary planform - both flat and cambered - is illustrated in several examples. A simple local-sweep approximation is shown to provide reasonable estimates of thrust for certain classes of flat wings of arbitrary planform and to permit the design of a wing leading edge for a specified thrust distribution.

INTRODUCTION

Leading-edge thrust is an important factor in the aerodynamic performance of wings at subsonic speeds. This force results from the upwash field ahead of the wing and the high local velocities and accompanying low pressures which occur as air flows around the wing leading edge to the upper surface from a stagnation point on the undersurface. The high aerodynamic efficiency of wings of large aspect ratio depends directly on the presence of leading-edge thrust to counteract the drag arising from pressure forces acting on the remainder of the airfoil. Leading-edge thrust for subsonic speeds may be predicted by a variety of methods including a vortex-lattice computer program (refs. 1 and 2) capable of handling wings of complex planform with twist and camber.

At supersonic speeds, however, leading-edge thrust plays a substantially reduced role. In relation to other forces acting on the wing, the thrust continually decreases with increasing speed until the Mach number normal to the leading edge becomes sonic, at which point, upwash ahead of the wing leading edge is reduced to zero and thrust is no longer developed. Furthermore, even for conditions where a substantial amount of leading-edge thrust is theoretically possible, it often happens that little of the thrusting force develops because the flow cannot remain attached to the relatively sharp airfoils often employed for supersonic flight.

Nevertheless, thrust considerations do play a significant role in the analysis of wings at supersonic speeds. For low supersonic speeds and for wings with well-rounded leading edges an appreciable percentage of theoretical leading-edge thrust may be developed. Furthermore, Polhamus (ref. 3) has shown that when the thrust fails to develop because of detached flow the effects are not necessarily dissipated. If the flow reattaches these effects can reappear in an associated phenomena, the formation of a leading-edge vortex flow. For supersonic as well as subsonic speeds, the influence of this flow breakdown on wing lift and drag may be estimated by application of the Polhamus leading-

edge-suction analogy, which operates vectorially on the theoretical leading-edge thrust.

Supersonic wings with straight-line leading edges may be treated analytically by use of classical linearized theory (refs. 4, 5, and 6). However, for other wing planforms of interest (wings with cranked or curved leading edges) theoretical methods are not available and numerical methods are required. Such a method, described in reference 7, provided the groundwork for development of an improved system reported in this paper. The primary advantage of the newer method lies in elimination of the need for user examination and fairing of program-generated pressure distributions, which accordingly provides for a much higher degree of automation. In addition, this improved method does not require pressure data beyond the immediate vicinity of the leading edge and thus permits a better definition of thrust distribution for wings with a complex leading edge.

The new method for evaluation of theoretical leading-edge thrust has been programmed as an extension to an existing high-speed digital computer method for prediction of wing loading distributions described in reference 8. In addition to the leading-edge thrust distributions the present modified program provides lift and drag estimates based either on theoretical leading-edge thrust or on employment of the Polhamus suction analogy. An application of empirical estimates of the percentage of leading-edge thrust actually attainable as given in reference 9 may permit more exact predictions of wing aerodynamic performance.

Additional considerations discussed herein provide a means of designing a wing planform to provide (within limits) a specified thrust distribution. This capability should be useful in attempts to avoid leading-edge separation and obtain as much of the theoretical leading-edge thrust as is practically possible.

SYMBOLS

b wing span

c_a average wing chord, $\frac{S}{b}$

C_D wing drag coefficient

$\Delta C_{D,A}$ drag-coefficient increment due to a separated leading-edge vortex according to Polhamus analogy (see eq. (10))

$\Delta C_{D,T}$ drag-coefficient increment due to theoretical leading-edge thrust (see eq. (8))

C_L wing lift coefficient

$\Delta C_{L,A}$ lift-coefficient increment due to a separated leading-edge vortex according to Polhamus analogy (see eq. (11))

$\Delta C_{L,T}$ lift-coefficient increment due to theoretical leading-edge thrust (see eq. (9))

C_N wing normal-force coefficient

ΔC_p lifting pressure coefficient

$\Delta C_{p,P}$ lifting pressure coefficient defined by numerical program

$\Delta C_{p,Th}$ lifting pressure coefficient defined by linearized theory

$\Delta C_p\sqrt{x'}$ leading-edge singularity parameter

$\left(\Delta C_p\sqrt{x'}\right)_o$ limiting value of leading-edge singularity parameter at $x' = 0$

C_t section thrust coefficient, $\frac{t}{qc_a}$

C_T wing thrust coefficient, $\frac{2}{b}\int_0^{b/2} C_t \, dy$

$E(k)$ elliptic integral of second kind with modulus k

e exponent used in definition of empirical function, $F(x'_m)$

$F(x'_m)$ empirical function providing for correction of numerical method pressure coefficient location. See equations (14) to (16) in appendix and section entitled "Numerical Method Development."

k modulus of elliptic integral, $\sqrt{1 - \beta^2 \cot^2 \Lambda}$

k_o modulus of elliptic integral for $\Lambda = \Lambda_o$, $\sqrt{1 - \beta^2 \cot^2 \Lambda_o}$

k_1, k_2, k_3, k_4 constants used in singularity-parameter curve fit or in definition of empirical function $F(x'_m)$

M Mach number

n integers designating terms in summations

q dynamic pressure

S wing area

t section leading-edge thrust

V free-stream velocity

x,y,z Cartesian coordinates with origin at wing apex, x measured along wing root chord

x' distance behind leading edge at which lifting pressure is assumed to act, in program units (see ref. 8)

x'_m distance behind leading edge of midpoint of a program element (see ref. 8)

y_o wing span position for initiation of constant thrust design

α angle of attack, degrees

β $= \sqrt{M^2 - 1}$

δ angle at a cambered-wing leading edge between a tangent to surface and angle-of-attack reference plane, $\tan^{-1} \frac{dz}{dx}$

Λ leading-edge sweep angle

Λ_o leading-edge sweep angle at y_o

ρ air density

THEORETICAL CONSIDERATIONS

The magnitude of the leading-edge thrust developed by a thin lifting wing is dependent on the upwash just ahead of the leading edge and on the airfoil camber surface just behind the leading edge. The influence of both of these factors is reflected in the pressure distribution in the vicinity of the leading edge. For a lifting wing with subsonic leading edges (leading-edge sweep angle greater than $\tan^{-1} \sqrt{M^2 - 1}$) the upwash given by linearized theory is infinite at the leading edge, and the pressure at the leading edge is also infinite unless the wing has a camber surface designed specifically to avoid such a singularity. In spite of these singularities, there is a measure of the influence of upwash and camber effects on the leading-edge thrust; it is given by the limiting value at the leading edge of the singularity parameter $\Delta C_p \sqrt{x'}$. Hayes in reference 4 gives an expression for leading-edge thrust per unit distance in the spanwise direction which, when transformed to the symbols of this report, is

$$t = \frac{\pi \rho V^2}{16} \tan \Lambda \sqrt{1 - \beta^2 \cot^2 \Lambda} \left(\Delta C_p \sqrt{x'} \right)_o^2 \qquad (1)$$

A section thrust coefficient will be defined as

$$C_t = \frac{\pi}{8} \frac{b}{S} \tan \Lambda \sqrt{1 - \beta^2 \cot^2 \Lambda} \left(\Delta C_p \sqrt{x'}\right)_o^2 \tag{2}$$

where the average wing chord c_a rather than the local chord was chosen as a reference in order to preserve the linear nature of the thrust distribution for delta wings.

The central problem is the evaluation of the limiting value of the singularity parameter $\left(\Delta C_p \sqrt{x'}\right)_o$. For flat wings with cranked or curved leading edges and for cambered wings of any planform numerical methods must be employed. The methods employed in this paper are discussed at some length in the section entitled "Numerical Method Development." For a certain class of wings, flat wings with straight leading edges, analytic solutions are available. These solutions are also valuable in checking the validity of numerical methods, and in this paper will be used for that purpose.

Through use of relationships given in reference 6, the limiting value of the singularity parameter for a flat delta wing at a small angle of attack may be expressed as

$$\left(\Delta C_p \sqrt{x'}\right)_o = \frac{4 \sin \alpha}{\sqrt{2}} \frac{\sqrt{y \cot \Lambda}}{E(k)} \tag{3}$$

where

$$k = \sqrt{1 - \beta^2 \cot^2 \Lambda}$$

The section leading-edge thrust coefficient for a flat delta wing is then

$$C_t = \pi \sin^2 \alpha \frac{b}{S} y \frac{\sqrt{1 - \beta^2 \cot^2 \Lambda}}{\left[E(k)\right]^2} \tag{4}$$

and the total thrust coefficient for the wing becomes

$$C_T = \int_0^{b/2} C_t \, dy = \pi \sin^2 \alpha \frac{b^2}{4S} \frac{\sqrt{1 - \beta^2 \cot^2 \Lambda}}{\left[E(k)\right]^2} = \pi \sin^2 \alpha \cot \Lambda \frac{\sqrt{1 - \beta^2 \cot^2 \Lambda}}{\left[E(k)\right]^2} \tag{5}$$

The lifting force acting normal to the wing surface may be expressed in coefficient form as

$$C_N \approx 2\pi \sin \alpha \frac{\cot \Lambda}{E(k)}$$

and thus the thrust force may be related to the normal force by

$$\frac{C_T}{C_N} \approx \frac{\sin \alpha}{2} \frac{\sqrt{1 - \beta^2 \cot^2 \Lambda}}{E(k)}$$

In figure 1, the theoretical relationships have been used to illustrate the relative importance of the leading-edge thrust for delta wings of several sweep angles operating over a speed range up to $M = 2.5$. Data for the subsonic portion of the speed range were obtained from reference 10. The component of the thrust opposing the drag, $C_T \cos \alpha$, is given as a fraction of drag component of the normal force, $C_N \sin \alpha$. At very low speeds, as would be expected, the fraction approaches 1 as the sweep angle decreases and the aspect ratio increases. It is interesting to note that at $M = 1.0$, the theory indicates that the value of the component of thrust opposing drag is one-half the value of the drag component of the normal force for all leading-edge sweep angles. With increasing supersonic Mach numbers, there is a steady reduction in the theoretical thrust until the leading edge becomes supersonic, at which point the thrust becomes and remains zero. Below a Mach number of 1 the lower sweep angles provide the highest thrust, but at supersonic speeds the more highly swept wings provide the greater relative thrust levels. The section leading-edge thrust coefficient of a delta wing defined by equation (4) may also be used in a "local sweep approximation" applicable to flat wings of arbitrary planform which do not depart drastically from a straight-line leading edge. For this purpose, Λ is the local sweep angle and S and b refer to the arbitrary-planform wing. Sketch (a) illustrates the application of the local sweep approximation to a

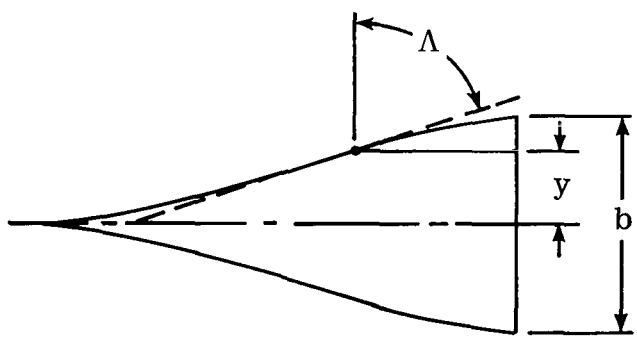

Sketch (a)

wing of "ogee" planform. As will be discussed later, this approximation has been used to help verify program results for wings of arbitrary planform. The approximation may also be useful in the design of wing leading edges to produce a given leading-edge thrust. This capability could be useful in attempts to avoid leading-edge separation and obtain as much of the theoretical leading-edge thrust acting in the chord plane of the wing as is practically possible. Since, in general, the thrust is small for inboard span positions, the design process

will be used only outboard of some selected span position y_o which has been determined to have an acceptable thrust-level (upwash magnitude) for the retention of attached flow. The local-sweep approximation form of equation (4) may be used to define a sweep angle Λ at a span position y outboard of y_o which will keep the thrust constant. The expression used is

$$\frac{k}{[E(k)]^2} = \frac{y_o}{y} \frac{k_o}{[E(k_o)]^2} \tag{6}$$

where $k = \sqrt{1 - \beta^2 \cot^2 \Lambda}$ and $k_o = \sqrt{1 - \beta^2 \cot^2 \Lambda_o}$ in which Λ_o is the sweep angle at y_o. The required value of Λ must be found by iteration. When new Λ-values have been found for a series of span stations from y_o to the wing tip, the leading edge may be defined by a numerical integration of

$$x = \int_0^y \tan \Lambda \, dy \tag{7}$$

In examples of leading-edge planform design given in this paper, the iterations were performed by a programmable handheld calculator. The following approximation for the elliptic integral was found to be useful for that purpose:

$$E(k) \approx 1 + \left(\frac{\pi}{2} - 1\right)(\beta \cot \Lambda)^{\eta}$$

where

$$\eta = 1.226 + 0.15\pi(1-\sqrt{\beta \cot \Lambda})$$

This expression is accurate within about 0.02 percent over the full $\beta \cot \Lambda$ range of 0 to 1.

For wings of arbitrary planform and surface shape, the section thrust coefficient defined by equation (2) (with a numerically determined value of singularity parameter) may be used to estimate the influence of thrust on wing lift and drag. For theoretical leading-edge thrust the incremental lift and drag coefficients due to thrust at a given angle of attack may be expressed as

$$\Delta C_{D,T} = -\frac{2}{b} \int_0^{b/2} C_t \cos (\alpha - \delta) \, dy \tag{8}$$

$$\Delta C_{L,T} = \frac{2}{b} \int_0^{b/2} C_t \sin (\alpha - \delta) \, dy \tag{9}$$

For the Polhamus leading-edge-suction analogy these increments may be approximated as

$$\Delta C_{D,A} = -\frac{2}{b}\int_0^{b/2} C_t \frac{\sin(\alpha - \delta)}{\cos \Lambda}\, dy \tag{10}$$

$$\Delta C_{L,A} = \frac{2}{b}\int_0^{b/2} C_t \frac{\cos(\alpha - \delta)}{\cos \Lambda}\, dy \tag{11}$$

The thrust vector and its relationship to the wing leading edge is illustrated in sketch (b). As can be seen, the expressions for lift and drag increments

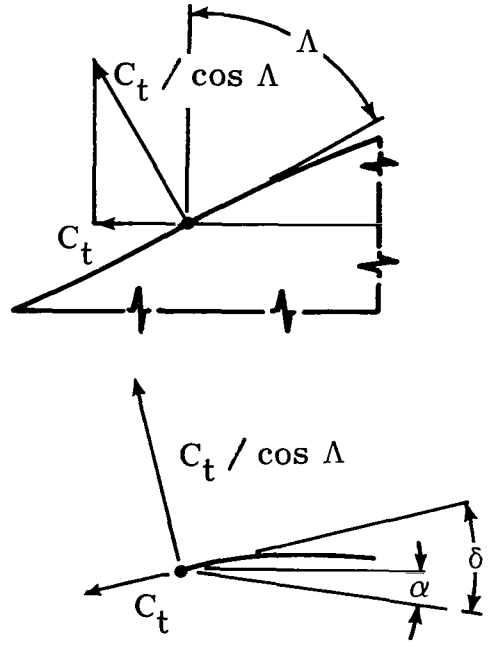

Sketch (b)

based on the Polhamus analogy are applicable only for small angles of attack and for small camber surface slopes. The section suction force vector, approximated as $C_t/\cos \Lambda$, is assumed to be rotated to act normal to the wing surface at the leading edge. For reattached leading-edge vortex flow, the vortex center would actually depend on the angle of attack and in general would be downstream of the leading edge. This downstream location is where the suction force vector should be applied if such a position could be established. Nevertheless, for mildly cambered wings at small angles of attack, the analysis used here should provide reasonable estimates of the effects of separated leading-edge vortex flow on wing lift and drag.

NUMERICAL METHOD DEVELOPMENT

The first requirement in the development of a numerical method for estimation of theoretical leading-edge thrust for wings of arbitrary planform is a sufficiently accurate definition of lifting pressures in the vicinity of the wing leading edge. These pressures are then used in determination of the limiting value of the singularity parameter $\left(\Delta C_p\sqrt{x'}\right)_o$. A computer program described in reference 8 provides theoretical pressure distributions for both flat and cambered wings of arbitrary planform.[1] In general, the program provides a reasonable description of the wing overall pressure distributions and of integrated forces and moments. A particular shortcoming of the program, however, has been a tendency toward oscillation of pressure values which unfortunately is accentuated near the leading edge. In view of the theoretical singularity in pressure at the leading edge, this is likely to be a characteristic of any numerical method based on linearized theory. In this section, means of employing the theoretical pressure distributions generated by the computer program of reference 8 to obtain leading-edge-thrust estimates of reasonable accuracy are explored. First, a study of flat-wing characteristics is made, and then attention is given to the more general cambered-wing case.

Flat Wings

For flat wings with straight-line leading edges the theoretical lifting pressure near the leading edge may be approximated by the function

$$\Delta C_p = k_1 \frac{1}{\sqrt{x'}} + k_2\sqrt{x'}$$

in which the first term is dominant. A representative distribution of lifting pressure near the leading edge is shown in sketch (c). It is assumed that for

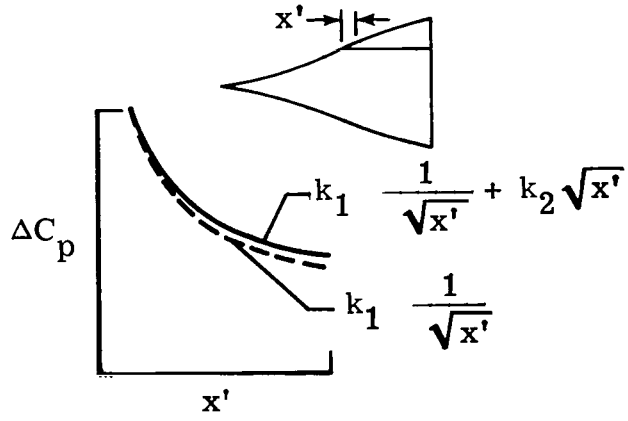

Sketch (c)

[1]An error in the program description given in reference 8, uncovered in the course of this study, is corrected in the appendix.

flat wings with cranked or curved leading edges, this approximation (with different constants of course) would still be appropriate. The corresponding function for the singularity parameter is

$$\Delta C_p\sqrt{x'} = k_1 + k_2 x'$$

which would appear as shown in sketch (d). Again the dominance of the first term is apparent. The second term, however, is valuable in determination of the limiting value of the singularity parameter if values of x' at an appreciable distance from the leading edge must be employed. With the form of the data established, a least-squares curve fit may be applied to program-generated data $\left(\Delta C_p\sqrt{x'}\right.$ as a function of $\left.x'\right)$ in order to find a representative limiting

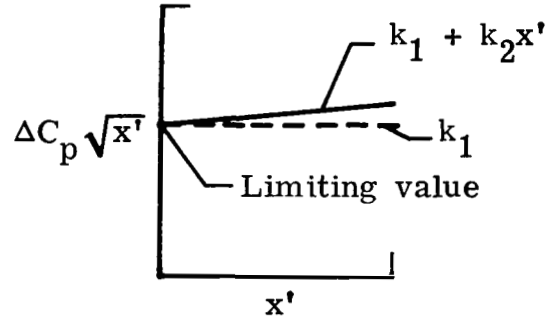

Sketch (d)

value of the singularity parameter at a given span station. For the loading approximation chosen

$$\Delta C_p\sqrt{x'} = \frac{\sum_0^n (x_n')^2 \sum_0^n \Delta C_p\sqrt{x_n'} - \sum_0^n x_n' \sum_0^n x_n' \left(\Delta C_p\sqrt{x'}\right)_n}{n\sum_0^n (x_n')^2 - \sum_0^n x_n' \sum_0^n x_n'} \tag{12}$$

An example of the application of the simple curve-fit function to pressure data generated by the program of reference 8 is given in figure 2. As in the description of the program given in reference 8, the lifting pressure for a given element is assumed to act at the element midpoint x_m'. The data cover the first three elements directly behind the leading edge at the mid-semispan location and at the span stations immediately inboard and outboard. These nine data points occupy less than 8 percent of the local chord. In the ΔC_p plot, the program-generated pressures are seen to provide what can be regarded as a reasonable agreement with the linearized theory. However, there are discrepancies; and, as can be better seen in the singularity-parameter plot, the program data range from about 25 percent above to about 20 percent below the

theoretical values. The least-squares curve fit of the singularity-parameter function $\Delta C_p\sqrt{x'} = k_1 + k_2 x'$ to the program data gives a limiting value of the parameter about 8 percent too high which, since $(\Delta C_p\sqrt{x'})_o$ is squared, translates to a 16-percent error in the local leading-edge thrust. Considerably larger errors occurred at other stations, and thus the simple approach illustrated here was abandoned.

The nature of the program errors depicted in figure 2 led to a further rather comprehensive study of these errors. Although errors in the vicinity of the leading edge were found to be quite large, they were found to display a remarkably organized character. As discussed in the appendix, it was found that the errors were dependent on only two quantities, the distance behind leading edge x' and the leading-edge sweep condition, $\beta \cot \Lambda$. A function $F(x'_m)$ describing the errors is presented in the appendix. An illustration of the systematic nature of the errors for the Mach number and sweep angle of the example of figure 2 is given in figure 3. The data shown here cover the first three elements behind the leading edge for wing span stations from 0.075b/2 (in increments of 0.025b/2) to points near the wing tip where program ΔC_p data were invalidated by the proximity of the trailing edge and the tip Mach cone. The data points displaying the largest departures from the general trend are for the more inboard stations. The organized behavior of the errors appears to improve as the span station increases and the number of elements involved in the program solution increases. The empirical function $F(x'_m)$ applicable to this example is also shown. Small deviations between this function and the trend line of the data occur because of compromises in fitting of the function to the full range of $\beta \cot \Lambda$ values. The organized and predictable nature of the program ΔC_p errors allows the introduction of a correction based on the local sweep angle Λ and on the distance of the element midpoint behind the leading edge x'_m. The correction is applied to the location of the lifting pressure coefficient rather than to the pressure itself. The choice of the element midpoint for the pressure location is after all only an assumption. Furthermore, such a shift in location only will have little influence on the lifting pressure distribution for cambered wings at or near design condition (a topic to be discussed later). By using the assumption that ΔC_p varies inversely with the square root of the distance behind the leading edge, a corrected lifting-pressure location is found as follows: The corrected pressure at x'_m is $\Delta C_p / F(x'_m)$ so that

$$\frac{\Delta C_p / F(x'_m)}{\sqrt{x'_m}} = \frac{\Delta C_p}{\sqrt{x'}}$$

and

$$x' = \frac{x'_m}{F(x'_m)^2}$$

or

$$x' = x'_m + \Delta x'$$

where

$$\Delta x' = x'_m \left[\frac{1}{F(x'_m)^2} - 1 \right]$$

An illustration of the use of the empirical function $F(x'_m)$ in obtaining a corrected pressure location is given in figure 4. As would be expected, the correlation of the adjusted program data with the theory is much improved.

The significant point, however, is not that in this one particular instance an improved numerical result was obtained, but that such results are representative of those obtained over a large range of Mach number/leading-edge-sweep conditions. Although the empirical function, and the correction it affords, is based on wings with straight-line leading edges, it is believed to be applicable to wings with cranked or curved leading edges also. In the immediate vicinity of a crank, the pressure distribution may not be typical of that for straight-line leading edges; but such flow patterns should be established to an increasing degree as the distance from the crank increases, and more readily for small cranks than for large ones. A curved leading edge is treated as a succession of cranks which must necessarily be small, and the correction should be applicable here too.

The behavior of the leading-edge singularity parameter $\Delta C_p\sqrt{x'}$ for the adjusted pressure data is illustrated in figure 5. Now a least-squares curve fit of the function $\Delta C_p\sqrt{x'} = k_1 + k_2 x'$ yields a limiting singularity parameter within about 1 percent of the theoretical value. A further illustration of the improvement afforded by the empirical pressure-location adjustment is given by the spanwise thrust distribution of figure 6. Program section thrust coefficients are found by inserting limiting singularity-parameter values defined by equation (12) into the expression for section thrust coefficient, equation (2). Program results for which x' was defined by the empirical function follow very closely the linearized-theory distribution line, whereas program results obtained without the adjustment display a very erratic behavior.

The empirical function $F(x'_m)$ used to provide adjusted pressure-coefficient locations was defined as outlined in the appendix from program pressure data for a large range of $\beta \cot \Lambda$ values, 18 in all. Program thrust coefficients for that series of $\beta \cot \Lambda$ values would thus be expected to correlate well with the thrust given by linearized theory. In order to test the general applicability of the numerical method, correlations of program and theoretical thrust distributions have been made for delta wings with other $\beta \cot \Lambda$ values. A sample is given in figure 7. Only for small values of $\beta \cot \Lambda$ is any difficulty encountered. For these small values, the entire leading edge is represented by a small number of elements (12 for $\beta \cot \Lambda = 0.13$, for example). Total thrust coefficients for a series of flat delta wings covering a large range of $\beta \cot \Lambda$ values are given in figure 8. None of the $\beta \cot \Lambda$ values shown here corresponds to those used in generation of the empirical function $F(x'_m)$. The numerical-method/linearized-theory correlation appears to be acceptable over the full $\beta \cot \Lambda$ range.

Cambered Wings

For cambered wings, wings with any departures from a perfectly flat lifting surface, the numerical method just described is not completely adequate. It is the usual practice in the design of cambered wing surfaces for supersonic speeds (ref. 8, for instance) to define a camber surface which will produce the desired lift with pressure loadings having no leading-edge singularity. At the design lift coefficient, typical lifting pressure distributions near the leading edge may be approximated by a two-term function

$$\Delta C_p = k_3 + k_4 x'$$

as illustrated in sketch (e). Even for camber surfaces which are not designed in such a fashion, there is likely to be some angle of attack at which loadings near the leading edge at a given span station display this behavior. As shown in sketch (f), the limiting value of the leading-edge singularity parameter for this loading is zero, and there is no leading-edge thrust.

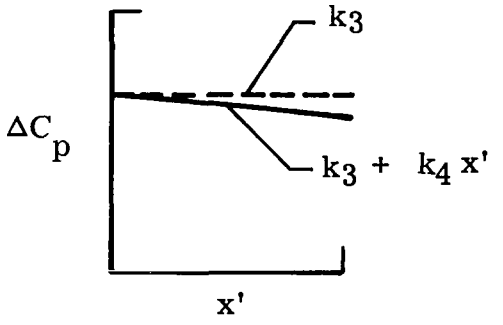

Sketch (e)

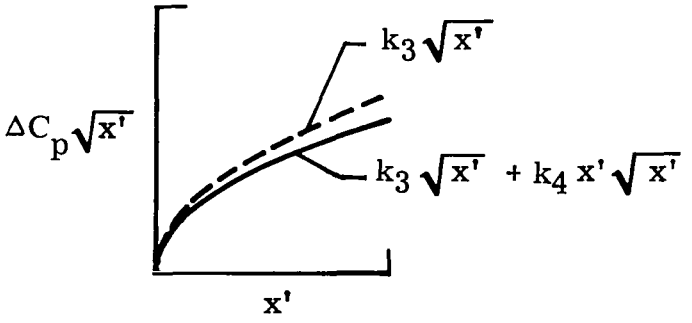

Sketch (f)

At any given span station, there is only one wing angle of attack that can produce a loading without singularities, and that angle of attack may be different for every span station. For any other angle of attack, the loadings will be composed of camber-design-point and flat-plate contributions, and thus singularities and leading-edge thrust will reappear. Using the two terms of both the

cambered and flat-plate loadings the singularity parameter function can be expressed as

$$\Delta C_p\sqrt{x'} = k_1 + k_2x' + k_3\sqrt{x'} + k_4x'\sqrt{x'}$$

As will be shown subsequently, this four-term function when employed in a least-squares fit of the program data leads to severe numerical instabilities. Thus, as a compromise, only the first term of the flat-wing loading and the first term of the cambered-wing loading was retained, and the singularity parameter for a cambered wing was expressed as

$$\Delta C_p\sqrt{x'} = k_1 + k_3\sqrt{x'}$$

The leading-edge singularity parameter functions for the cambered wing are illustrated in sketch (g). For the loading approximation chosen, the limiting

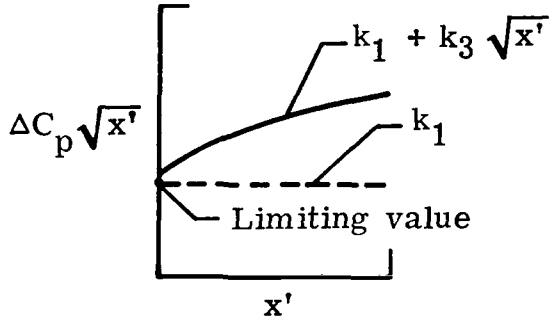

Sketch (g)

value of the singularity parameter defined by a least-squares curve fit is

$$\left(\Delta C_p\sqrt{x'}\right)_o = \frac{\sum_0^n x_n' \sum_0^n \left(\Delta C_p\sqrt{x'}\right)_n - \sum_0^n \sqrt{x_n'} \sum_0^n \sqrt{x_n'}\left(\Delta C_p\sqrt{x_n'}\right)_n}{n\sum_0^n (x_n')^2 - \sum_0^n \sqrt{x_n'} \sum_0^n \sqrt{x_n'}} \qquad (13)$$

An example of the application of the cambered-wing curve-fit functions to pressure data generated by the program of reference 8 for a three-loading cambered wing designed by a program method also described in reference 8 is given in figure 9. The camber surface was designed to produce a lift coefficient of 0.125 at $M = 2$ for a reference angle of attack of 0^o. Both the pressure-coefficient and the singularity-parameter plots seem to indicate a small amount of flat-plate loading at the design condition. This is possible inasmuch as the camber surface is also designed by a numerical process which cannot be assumed to be exact. The two-term cambered-wing curve yields a reasonable value for the limiting value of the singularity parameter, but the four-term curve does not.

A further examination of the program thrust results for a cambered wing at design conditions is afforded in the thrust distribution shown in figure 10. Results for the four-term curve-fit expression are obviously erratic. When a least-squares curve fit is to be used for extrapolation, care must be taken in selection of the curve-fit equation. A large number of terms will reduce the errors at the specific data points but may easily produce curves which do not reflect the general character of the data. Program results for the much simpler two-term curve-fit expression are relatively well behaved. Except in the region of the wing tip, where numerical results are affected by a diminishing number of data points, there is a general trend of the program to asymptotically approach a section thrust coefficient of zero (the design goal) as the span position increases. This is to be expected, because a given amount of wing-lifting-surface curvature is spread over a larger number of chordwise wing elements as the spanwise distance increases. This benefits the wing design program in definition of the camber surface and evaluation program in the definition of pressures. Although the program thrust coefficients do not fully meet the design goal and are not identically zero, for the outboard portion of the wing they are small relative to the thrust coefficients for a flat wing of the same planform at an angle of attack of 1°. Perhaps of more significance, is the observation that the cambered-wing thrust is very small compared to the thrust produced by a flat-plate wing of the same planform developing the same lift (the linearized-theory curve for a flat wing at $\alpha = 4^{\circ}$; $C_L = 0.125$).

The numerical method for evaluation of cambered-wing leading-edge thrust must be capable of handling any camber surface including, as a special case, a perfectly flat lifting surface. This consideration, in addition to the flat-wing contribution to the loading of cambered wings at off-design conditions, necessitates an examination of the program results for flat wings when such a wing is treated as a cambered wing. It will be recalled that for a cambered wing the singularity parameter function is taken as $\Delta C_p\sqrt{x'} = k_1 + k_3\sqrt{x'}$ instead of the flat-wing function $\Delta C_p\sqrt{x'} = k_1 + k_2x'$. In figure 11 an example is given of the program thrust distribution for a flat wing treated as if it were a cambered wing. Program results are seen to be only slightly poorer than for the flat-wing treatment shown in figure 6. The correlations shown here are typical of those over a large range of $\beta \cot \Lambda$ values. It would have been possible to treat all wings, flat and cambered, using the cambered-wing curve fit; but because of the improved results and the relatively small programming complications, flat wings were chosen to be considered as a special class.

Program thrust distribution for the same cambered wing at several angles of attack is shown in figure 12. The thrust at $\alpha = 0^{\circ}$ is seen to be small compared to the thrust for the other angles of attack. For all three angles the program thrust is above the design goal, leading to the speculation that at the design condition the cambered wing surface has a small amount of flat-wing character not called for in the design. Although there are some irregularities, the program results for all the angles of attack are generally linear.

Total thrust coefficient as a function of lift coefficient for both the cambered wing and a flat-plate wing of the same planform is shown in figure 13. The program results for the cambered wing show that it came reasonably close to meeting the design thrust goals. The difference between the program-indicated

thrust and the design goal corresponds to a lift-coefficient increment of 0.016 (or about 0.5°) which is about one-eighth of the design lift coefficient.

PROGRAM DESCRIPTION

The numerical method for evaluation of leading-edge thrust has been incorporated into the program for analysis of wings at supersonic speeds described in reference 8. Only relatively minor program changes were required. The handling of program input data, the program generation of local pressure coefficients, and the integrations to obtain forces and moments (with leading-edge thrust excluded) remain as before. The primary additions are:

(1) A short routine (12 statements) for the calculation and storage of local leading-edge sweep angles expressed as $\beta \cot \Lambda$.

(2) A more lengthy routine (153 statements) for the calculation and storage of leading-edge thrust parameters as a function of angle of attack and span position.

(3) A routine (37 statements) for the recall of thrust parameters and program-calculated wing area and the calculation of thrust coefficients and lift and drag coefficients for theoretical leading-edge thrust as well as for the Polhamus analogy.

The key new routine is the second of those listed. It calculates adjusted pressure-coefficient locations for three elements behind the leading edge at the span station being considered and at one station on either side (a total of nine elements). In doing this, the routine first cycles through angles of attack (-4° to 6° for the cambered wing and 1° for the flat wing) and the full range of span positions to recover pressure coefficients. The adjusted pressure-coefficient locations are given by

$$x' = \frac{x'_m}{F(x'_m)^2}$$

where x'_m is the element midpoint and $F(x'_m)$ is a function of x'_m and $\beta \cot \Lambda$ defined in the appendix. Data points are discarded if x'_m is less than 0.1, because the adjustment becomes unreliable at small values of x'_m as $F(x'_m)$ approaches zero. Data points are discarded also if the pressure coefficients (with the program integral smoothing discussed in ref. 8) are affected by the proximity of the wing trailing edge or the Mach line from the leading edge of the tip chord. Under those conditions the empirical function $F(x'_m)$ is no longer applicable. From the remaining data points leading-edge singularity parameters $\Delta C_p\sqrt{x'}$ are then calculated and, as discussed in the section "Numerical Method Development," the limiting value of the singularity parameter is found by a least-squares fit of the equations

$$\Delta C_p\sqrt{x'} = k_1 + k_3\sqrt{x'}$$

for the cambered wing and

$$\Delta C_p\sqrt{x'} = k_1 + k_2 x'$$

for the flat wing. Numerically these limiting values are found by application of equation (12) for the flat wing and equation (13) for the cambered wing. A thrust-coefficient parameter $(\pi/8) \tan \Lambda\sqrt{1 - \beta^2 \cot^2 \Lambda}(\Delta C_p\sqrt{x'})_o^2$ is then calculated and stored. The thrust coefficient itself cannot be calculated at this point in the program because the wing area is as yet unknown. If the number of terms n in the least-squares summation is less than four, the limiting value of the leading-edge singularity parameter and the thrust-coefficient parameter are not calculated; instead, the thrust-coefficient parameter is determined from a linear least-squares extrapolation of the previously calculated thrust-coefficient parameters for the previous three inboard span stations. At the same time the thrust-coefficient parameter is calculated, similar parameters for later use in determination of wing lift and drag increments by means of equations (8) to (11) are calculated and stored.

The other program changes do not require elaboration. All of the output data of the previous program (for wings without leading-edge thrust) are retained. The revised program also provides distributions of section thrust coefficient C_t for a cambered wing at selected angles of attack and distributions of C_t/α^2 for a flat wing. In addition, lift and drag coefficients are given for the flat wing and the cambered wing at selected angles of attack for both theoretical leading-edge thrust and the Polhamus leading-edge-suction analogy. Copies of the program in the form of card decks or tapes as desired may be purchased from COSMIC, 112 Barrow Hall, the University of Georgia, Athens, GA 30602.

PROGRAM APPLICATION

A series of examples has been prepared to illustrate the application of the program to wings with cranked and curved leading edges. For these examples there is no applicable theory by which to judge the program results. In the examples for flat wings, however, the local sweep approximation discussed in the section "Theoretical Consideration" will be of value in assessing results.

Thrust distributions for a flat wing with cranked leading edges are shown in figures 14 and 15. In figure 14, the wing outer panel is more highly swept and in figure 15 the inner panel is more highly swept. The Mach numbers were chosen to present for each wing an all-subsonic leading-edge condition and a mixed-subsonic-supersonic leading-edge condition.

In figure 14, the data for $M = 1.75$ shows an abrupt change in the thrust coefficient at the leading-edge break with only two or three points showing an appreciable degree of numerical instability. Outboard of the crank, the program thrust approaches that predicted by the local sweep approximation. It is surprising that the numerical results show this limit to be approached so quickly. For a Mach number of 2.75, the inner panel has a supersonic leading edge and no

leading-edge thrust is developed. Beyond the break point, the program thrust approaches that given by the local sweep approximation but at a relatively slow rate.

In figure 15, at M = 1.75, where both panels have subsonic leading edges, numerical instabilities again appear to be restricted to two or three points in the vicinity of the break. Outboard of the break, the expected asymptotic approach to the local sweep approximation is observed. For a Mach number of 2.75 the program behavior is again as expected.

Program thrust distributions for a flat wing with a continuously curving leading edge are shown in figure 16. The "ogee" planform of this wing has a leading edge defined by

$$y = 0.13x + 0.715x^2 - 0.52x^3$$

Data are shown for three Mach numbers, one of which results in a mixed-subsonic-supersonic leading-edge condition. Here the local sweep approximation can be used only as a rough guide to aid in detection of gross program errors. Such errors do not appear to have materialized. It should be noted that at the wing tip, where the sweep angle is 90°, the local sweep approximation gives a thrust coefficient value of

$$C_t = \frac{\pi}{2} \alpha^2 \frac{b^2}{S}$$

for all Mach numbers, a value which appears to be approached by the program results.

In view of the preceding examples and others not presented in this paper, it is believed that the numerical procedures for evaluation of flat-wing leading-edge thrust are reasonably accurate. One somewhat surprising result of this study is the close agreement of the very simple local sweep approximation with the program results. This approximation appears to be reasonably accurate unless large changes in the local sweep angle (or a high degree of leading-edge curvature) are encountered. The approximation appears to be most accurate when changes in the local sweep angle may be considered to be small relative to the angular difference between the leading-edge sweep angle and the Mach-line sweep angle. Note that for the "ogee" wing example, the approximation is poor only for a Mach number of 2.5. Total thrust coefficients for the ogee wing are shown in figure 17 as a function of Mach number. Over the Mach number range in which the leading edge is everywhere subsonic, the local sweep approximation gives good results. At the highest Mach numbers the simple approximation may be in error by a factor of 2 or more. Where the error factors are large, however, the actual thrust levels are relatively small.

Because leading-edge thrust is now an easily obtained byproduct of the wing program used to evaluate pressure loadings and integrated forces for wings of arbitrary planform, there is little need for the local sweep approximation as

an evaluation tool. It may, however, be useful in design of leading-edge shapes for specified thrust distributions. Such a wing-planform design tool could be employed in attempts to delay to higher angle of attack the onset of separation-induced vortex flow and the associated drag penalties. Conversely, the design tool could equally well be employed in attempts to strengthen and stabilize a separation-induced vortex flow which tends to form at maneuver condition for highly swept wings. Examples of wing planform design for specified thrust distribution are shown in figure 18. A delta wing with 70° sweptback leading edge was the basic planform. For each of the three Mach numbers shown, the leading edge was altered from the mid-semispan position outboard to maintain a constant thrust level. Equation (6) was solved by iteration to define the required local sweep angle and the resultant leading-edge coordinates. The trailing-edge sweep angle was changed so as to preserve the area of the basic delta wing. Program results for the altered planforms agree reasonably well with the design goals. Experimentation is required to determine the practical benefits of such a design approach.

Program thrust distribution for a cambered wing of arbitrary planform is shown in figure 19. The wing design program of reference 8 was used to define a camber surface for an "ogee" wing whose planform was previously described. The surface was designed to produce a minimum drag at a Mach number of 2.0 and at a lift coefficient of 0.12. The camber surface was defined by an optimum combination of the first seven loadings of reference 8. It is seen that the thrust level for $\alpha = 0^{\circ}$, which corresponds to the design lift coefficient, is very low. At increasing angles of attack, although the program results display some oscillations, there is a generally smooth distribution which approaches the flat-plate results for this planform shown in figure 16. In this case there is no absolute way to judge program results; these results do, however, appear to be reasonable.

The numerical method also provides data for construction of lift-drag polars. First, this information is given for no leading-edge thrust, then data for the case of theoretical or 100-percent thrust are listed, and finally lift-drag data in which the Polhamus leading-edge-suction analogy has been applied are provided. Typical data for an "ogee" planform wing are shown in figure 20. Data for a flat wing, figure 20(a), show a significant reduction in drag if theoretical leading-edge thrust could be attained. The Polhamus analogy indicates higher drag values which are probably realistic estimates for such a wing with separation-induced vortex flow at the leading edge. The Polhamus analogy drag values are nevertheless lower than those of the upper curve for which the assumption of no thrust and no vortex lift was made. For the cambered "ogee," figure 20(b), the theoretical-thrust assumption and the Polhamus analogy give similar results for the effects of thrust at off-design conditions. Either curve should provide a reasonable estimate of the wing aerodynamic performance.

CONCLUDING REMARKS

A numerical method for the estimation of leading-edge thrust for supersonic wings of arbitrary planform has been developed and has been programmed as an extension to an existing high-speed digital computer method for prediction of wing pressure distributions. The accuracy of the method is assessed by compari-

son with linearized-theory results for a series of flat delta wings. Application of the method to wings of arbitrary planform - both flat and cambered - is illustrated in several examples. A simple local sweep approximation is shown to provide reasonable estimates of thrust for certain classes of flat wings of arbitrary planform and to permit the design of a wing leading edge for a specified thrust distribution. The program provides section thrust distributions and lift and drag for both flat and cambered wings of arbitrary planform. Results are given for theoretical leading-edge thrust and for application of the Polhamus leading-edge-suction analogy.

Langley Research Center
National Aeronautics and Space Administration
Hampton, VA 23665
August 3, 1978

APPENDIX

ANALYSIS OF ERRORS IN THE PROGRAM OF REFERENCE 8

As mentioned in the section entitled "Numerical Method Development," errors in lifting pressure coefficients calculated by the wing analysis program of reference 8 were found to display a remarkably organized character. These errors were studied by examining program ΔC_p data for a series of delta wings. It is the nature of the numerical method that pressure data for a given Mach number and leading-edge sweep angle are identical (except for the factor β) to that for all other Mach numbers and sweep angles for which the leading-edge sweep parameter $\beta \cot \Lambda$ remains a constant. Thus, it was possible to treat a very large number of Mach number/sweep-angle conditions by collecting data for a delta wing with a given sweep angle ($\Lambda = 70^\circ$) at a variety of Mach numbers. Because of the strong influence of local sweep conditions, this error analysis is believed to be applicable to wings of arbitrary planform provided the leading-edge curvature is small or that the point in question is at a sufficient distance from any breaks in the leading edge.

A sample of the distribution of program ΔC_p errors, the ratio of program to linearized-theory pressure coefficients, as a function of the distance behind the leading edge in program units is shown in figure 21. These representative data for 4 of the 18 $\beta \cot \Lambda$ values included in the study cover program unit span positions from 3 to the maximum permissible for a given $\beta \cot \Lambda$ value (integer value of 100 $\beta \cot \Lambda$ for $\beta \cot \Lambda$ less than 0.5 and 50 for $\beta \cot \Lambda$ greater than 0.5). Actually, because of the influence of the wing trailing edge and the wing-tip Mach line in alteration of pressure values, data for span positions in the immediate vicinity of the tip were in many cases discarded. For all values of $\beta \cot \Lambda$, the pressure coefficient ratio $\Delta C_{p,P}/\Delta C_{p,Th}$ appears to approach zero with decreasing values of x'_m. Because the pressure-location adjustment discussed in the section "Numerical Method Development" depends on the inverse square of this ratio, and because its approach to zero does not follow a precise pattern, adjustments for small values of x'_m are not reliable. Pressure data for x'_m less than 0.1 are discarded in the leading-edge-thrust evaluation process and these data are also omitted in figure 21. The very small $\beta \cot \Lambda$ values (0.096, for example) were included, not because delta wings with high sweep angles are of interest, but because high local sweep angles may be found on some wings of arbitrary planform.

For the range of practical sweep angles for delta wings, $\beta \cot \Lambda$ greater than 0.5, the program errors are relatively small (except just behind the leading edge) and damp out quickly with increasing distance from the leading edge. At small values of the $\beta \cot \Lambda$ parameter the errors become quite large and damp out much more slowly with increasing distance. However, it has been observed that for any given $\beta \cot \Lambda$ value (whether large or small) the errors follow a distinctive pattern. For the sample distributions shown here, the errors for a given $\beta \cot \Lambda$ fall into a relatively narrow band which can be approximated by an empirical function dependent only on x'_m.

The behavior of the pressure coefficient ratio $\Delta C_{p,P}/\Delta C_{p,Th}$ as a function of $\beta \cot \Lambda$ is shown in figure 22. Program data shown here have been obtained

for three selected x'_m values from fairings of curves of $\Delta C_{p,P}/\Delta C_{p,Th}$ as a function of x'_m such as those shown in figure 21. Again, it can be seen that although the errors become quite large, especially for small values of $\beta \cot \Lambda$, they display an orderly and predictable behavior.

The following set of equations were found to provide an adequate representation for an empirical function $F(x'_m)$ defining program errors to be expected at a given x'_m location for a given local sweep-angle condition $\beta \cot \Lambda$.

For $0.1 < x'_m \leq 0.5$

$$F(x'_m) = k_1\left(\frac{x'_m}{0.5}\right)^e \tag{14}$$

where

$$k_1 = \frac{1}{\sqrt{\beta \cot \Lambda}} + 0.22\sqrt{1 - \beta \cot \Lambda} - 0.22(1 - \beta \cot \Lambda) - 0.13(1 - \beta \cot \Lambda)^2$$

and

$$e = 0.32 + 0.25(\beta \cot \Lambda)^4$$

For $0.5 < x'_m \leq 1.5$

$$F(x'_m) = F(0.5) + k_1(x'_m - 0.5) + k_2(x'_m - 0.5)^2 + k_3(x'_m - 0.5)^3 \tag{15}$$

where $F(0.5)$ is an evaluation of equation (14) for $x'_m = 0.5$ and for $0.5 \leq \beta \cot \Lambda \leq 1.0$

$$k_1 = 0.33 - 1.96(1 - \beta \cot \Lambda) + 2.76(1 - \beta \cot \Lambda)^2$$

$$k_2 = -0.49 - 0.71(1 - \beta \cot \Lambda) - 1.42(1 - \beta \cot \Lambda)^2$$

$$k_3 = 0.09 + 2.42(1 - \beta \cot \Lambda) - 3.24(1 - \beta \cot \Lambda)^2$$

or for $0 \leq \beta \cot \Lambda \leq 0.5$

$$k_1 = 0.80 - 0.76/\sqrt{\beta \cot \Lambda/0.5}$$

$$k_2 = -1.80 + 0.60/\sqrt{\beta \cot \Lambda/0.5}$$

$$k_3 = 1.12 - 0.63/\sqrt{\beta \cot \Lambda/0.5}$$

For $1.5 < x_m' < 2.5$

$$F(x_m') = F(1.5) + k_1(x_m' - 1.5) + k_2(x_m' - 1.5)^2 + k_3(x_m' - 1.5)^3 \qquad (16)$$

where $F(1.5)$ is an evaluation of equation (15) for $x_m' = 1.5$ and for $0.5 \leq \beta \cot \Lambda \leq 1.0$

$$k_1 = 0.57 - 2.75(1 - \beta \cot \Lambda) + 8.02(1 - \beta \cot \Lambda)^2 - 9.28(1 - \beta \cot \Lambda)^3$$

$$k_2 = -0.94 + 4.90(1 - \beta \cot \Lambda) - 4.28(1 - \beta \cot \Lambda)^2 - 0.32(1 - \beta \cot \Lambda)^3$$

$$k_3 = 0.40 - 2.38(1 - \beta \cot \Lambda) - 1.51(1 - \beta \cot \Lambda)^2 + 7.90(1 - \beta \cot \Lambda)^3$$

or for $0.25 \leq \beta \cot \Lambda < 0.5$

$$k_1 = 0.04 - 8.88(0.5 - \beta \cot \Lambda) + 32.42(0.5 - \beta \cot \Lambda)^2 - 26.00(0.5 - \beta \cot \Lambda)^3$$

$$k_2 = 0.40 - 5.14(0.5 - \beta \cot \Lambda) + 51.79(0.5 - \beta \cot \Lambda)^2 - 144.12(0.5 - \beta \cot \Lambda)^3$$

$$k_3 = -0.18 + 11.05(0.5 - \beta \cot \Lambda) - 101.30(0.5 - \beta \cot \Lambda)^2 + 234.16(0.5 - \beta \cot \Lambda)^3$$

or for $0 < \beta \cot \Lambda < 0.25$

$$k_1 = 0.19 - 0.75/\sqrt{\beta \cot \Lambda/0.25}$$

$$k_2 = 0.14 - 0.04/\sqrt{\beta \cot \Lambda/0.25}$$

$$k_3 = -0.45 + 0.36/\sqrt{\beta \cot \Lambda/0.25}$$

These expressions have been programmed to provide the adjusted lifting pressure coefficient location discussed in the section "Numerical Method Development."

In the course of this study, an error in the description of the aft-element sensing technique for pressure-coefficient smoothing given in reference 8 was uncovered. For leading-edge elements the expression (eq. (33)) should have read:

$$\Delta C_p(L^*,N^*) = \frac{1}{2}\left[1 + \frac{A(L^*,N^*)}{1 + A(L^*,N^*)}\right]\Delta C_{p,a}(L^*,N^*) + \frac{1}{2}\left[\frac{1}{1 + A(L^*,N^*)}\right]\Delta C_{p,b}(L^*,N^*)$$

where for this purpose only, $A(L^*,N^*)$ is set equal to $A(L,N)$ for the same element. The error occurred in the program description and not in the program itself.

REFERENCES

1. Margason, Richard J.; and Lamar, John E.: Vortex-Lattice FORTRAN Program for Estimating Subsonic Aerodynamic Characteristics of Complex Planforms. NASA TN D-6142, 1971.

2. Lamar, John E.; and Gloss, Blair B.: Subsonic Aerodynamic Characteristics of Interacting Lifting Surfaces With Separated Flow Around Sharp Edges Predicted by a Vortex-Lattice Method. NASA TN D-7921, 1975.

3. Polhamus, Edward C.: Predictions of Vortex-Lift Characteristics by a Leading-Edge Suction Analogy. J. Aircr., vol. 8, no. 4, Apr. 1971, pp. 193-199.

4. Hayes, Wallace D.: Linearized Supersonic Flow. Ph. D. Thesis, California Inst. Technol., 1947.

5. Jones, Robert T.: Estimated Lift-Drag Ratios at Supersonic Speed. NACA TN 1350, 1947.

6. Puckett, A. E.; and Stewart, H. J.: Aerodynamic Performance of Delta Wings at Supersonic Speeds. J. Aeronaut. Sci., vol. 14, no. 10, Oct. 1947, pp. 567-578.

7. Sotomayer, William A.; and Weeks, Thomas M.: A Semi-Empirical Estimate of Leading Edge Thrust for a Highly Swept Wing in Supersonic Flow. AFFDL-TM-76-63-FXM, U.S. Air Force, Sept. 1976.

8. Carlson, Harry W.; and Miller, David S.: Numerical Methods for the Design and Analysis of Wings at Supersonic Speeds. NASA TN D-7713, 1974.

9. Sotomayer, W. A.; and Weeks, T. M.: Application of a Computer Program System to the Analysis and Design of Supersonic Aircraft. AIAA Atmospheric Flight Mechanics Conference, Aug. 1977, pp. 90-99. (Available as AIAA Paper No. 77-1131.)

10. Polhamus, Edward C.: Charts for Predicting the Subsonic Vortex-Lift Characteristics of Arrow, Delta, and Diamond Wings. NASA TN D-6243, 1971.

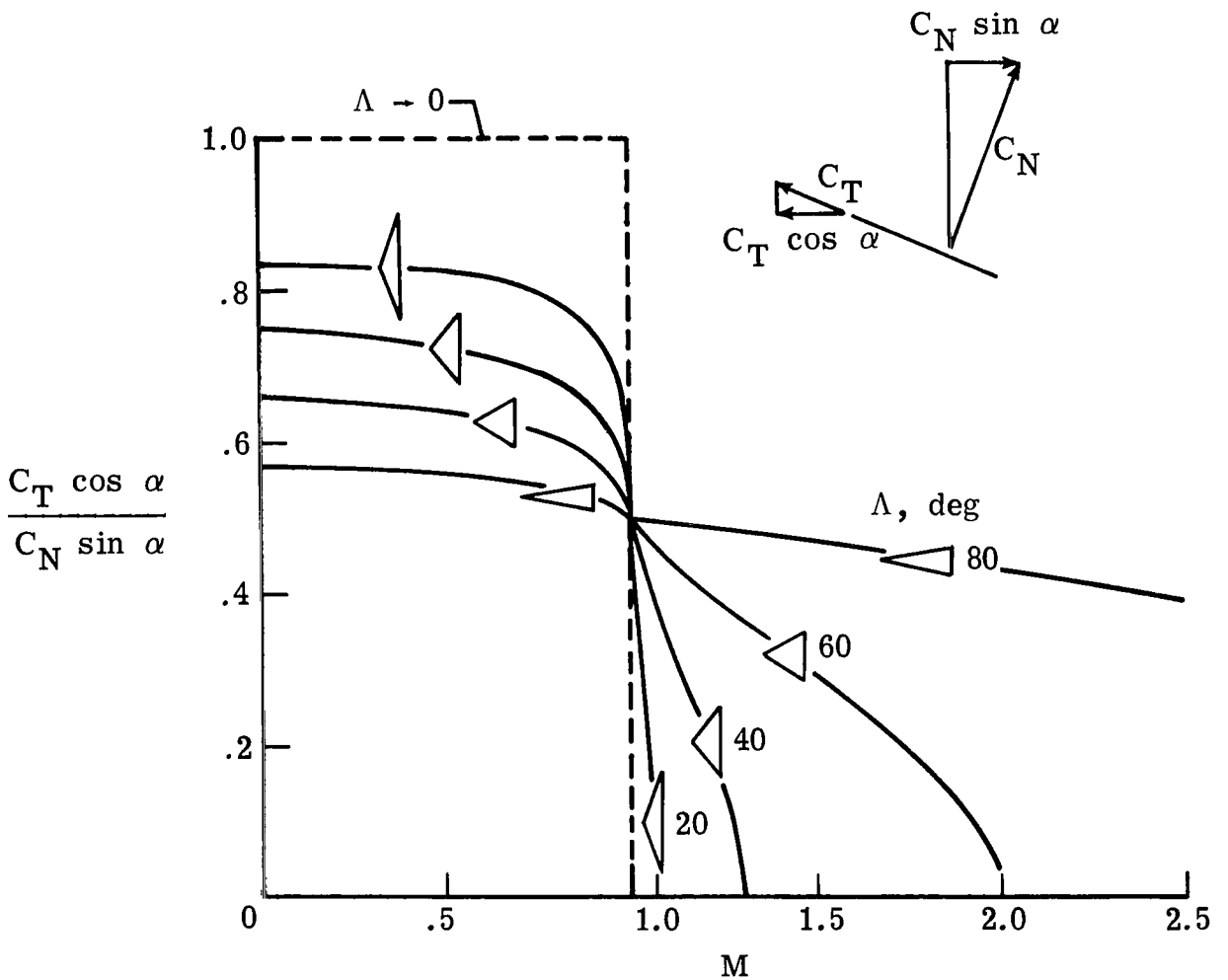

Figure 1.- The relative importance of leading-edge thrust at subsonic and supersonic speeds.

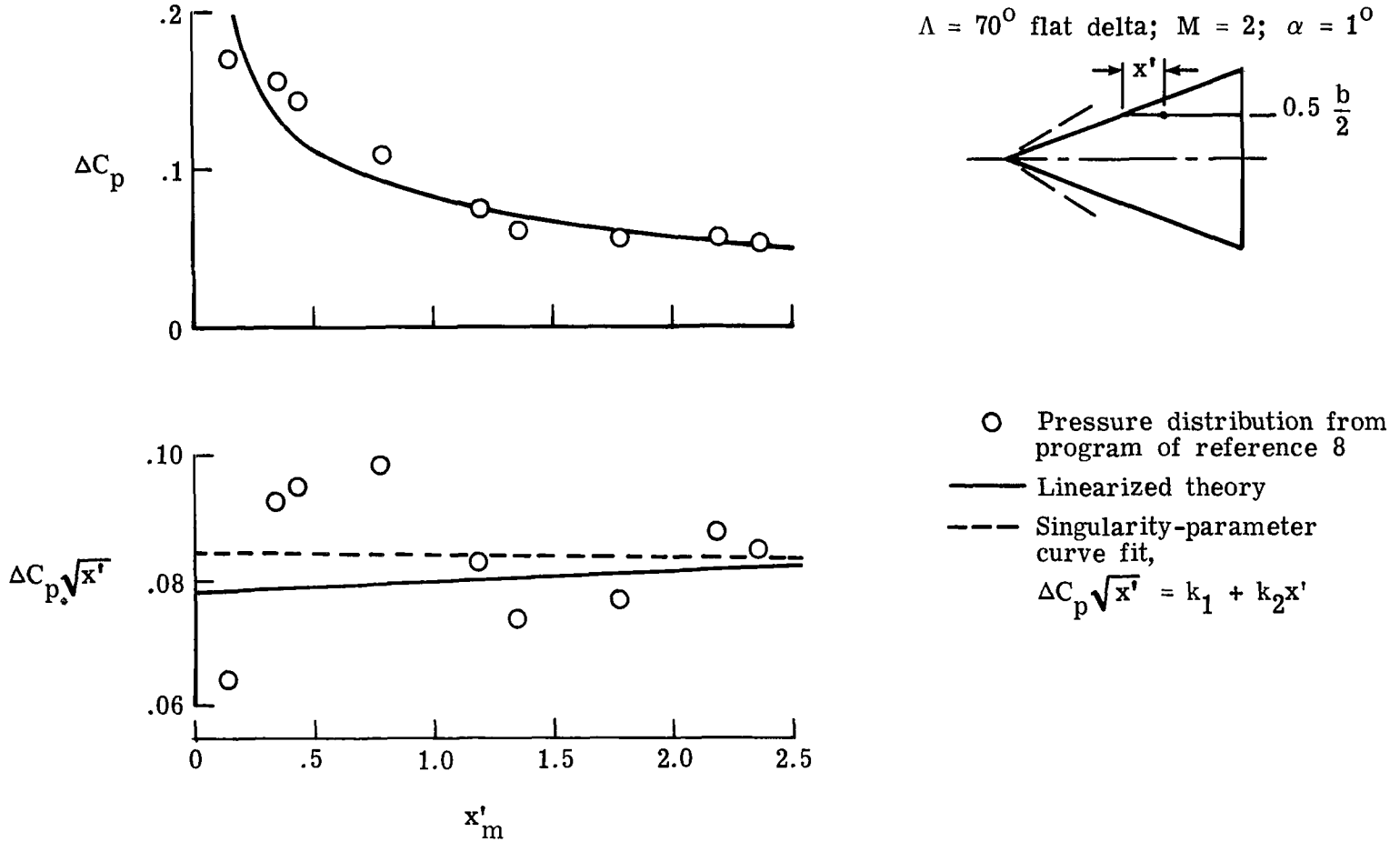

Figure 2.- An example of the direct application of a simple curve-fit function to pressure data generated by the program of reference 8.

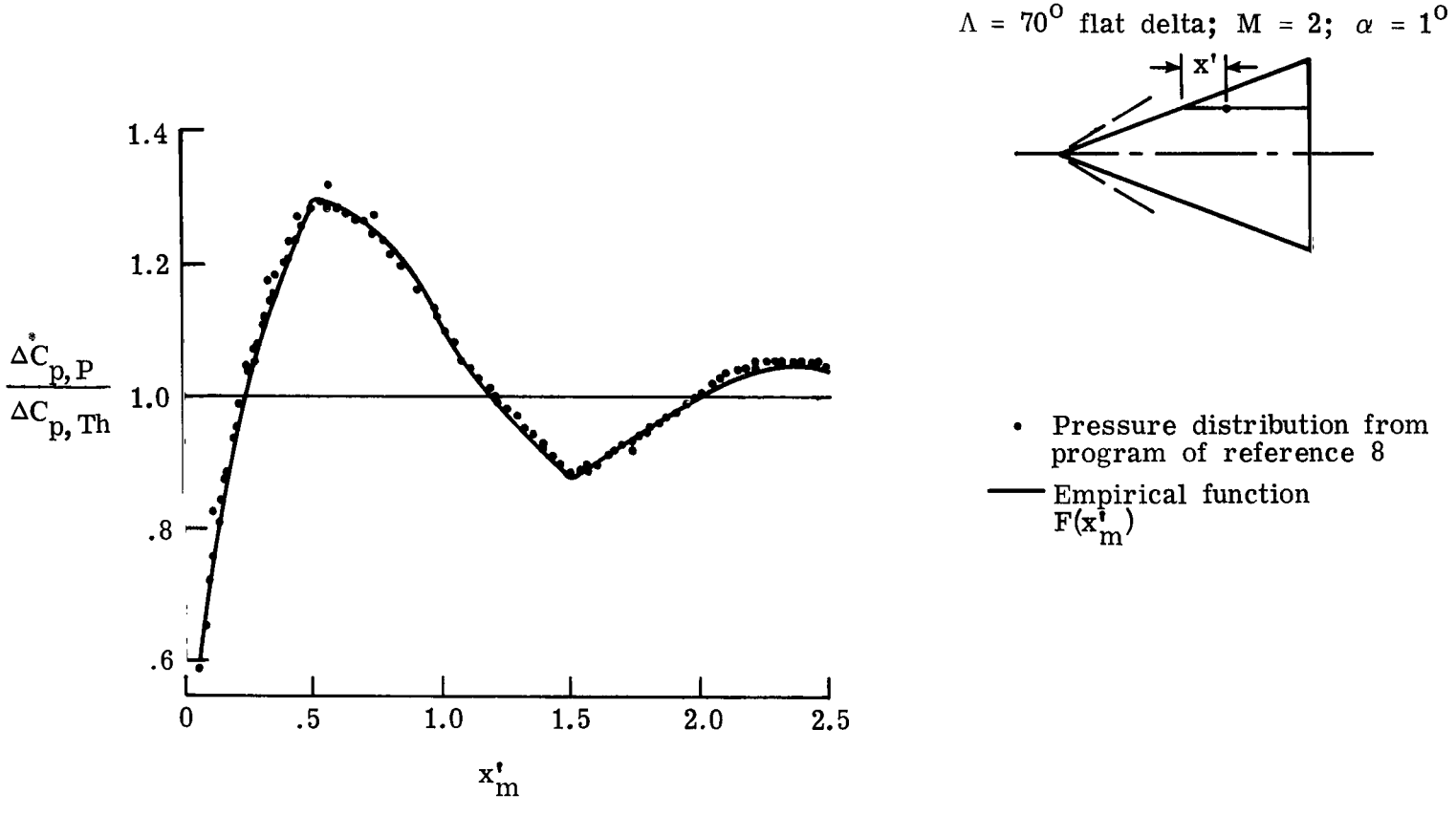

Figure 3.- An illustration of the systematic nature of the errors in the program of reference 8.

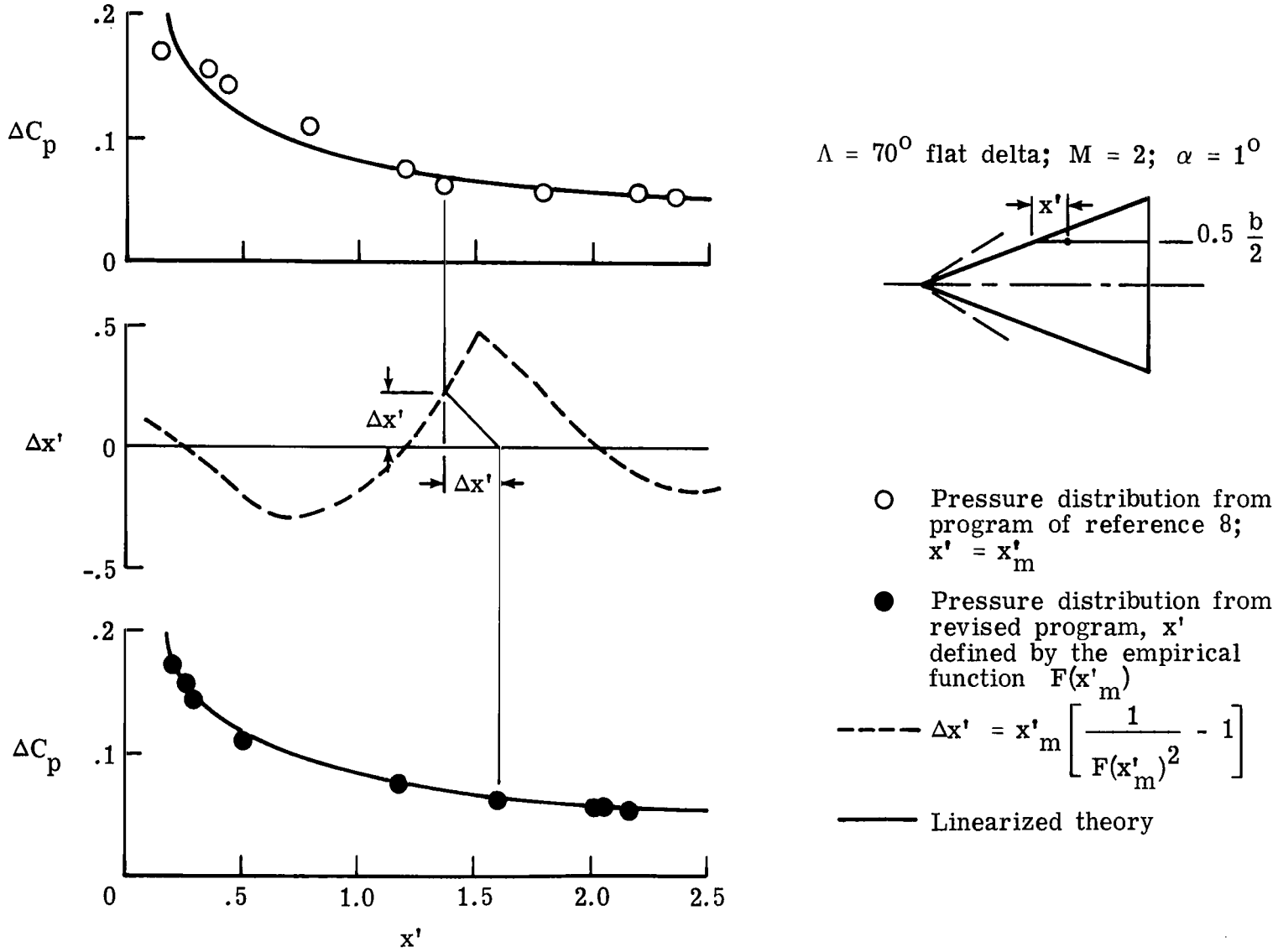

Figure 4.- An illustration of the use of the empirical function $F(x'_m)$ in obtaining a corrected pressure location.

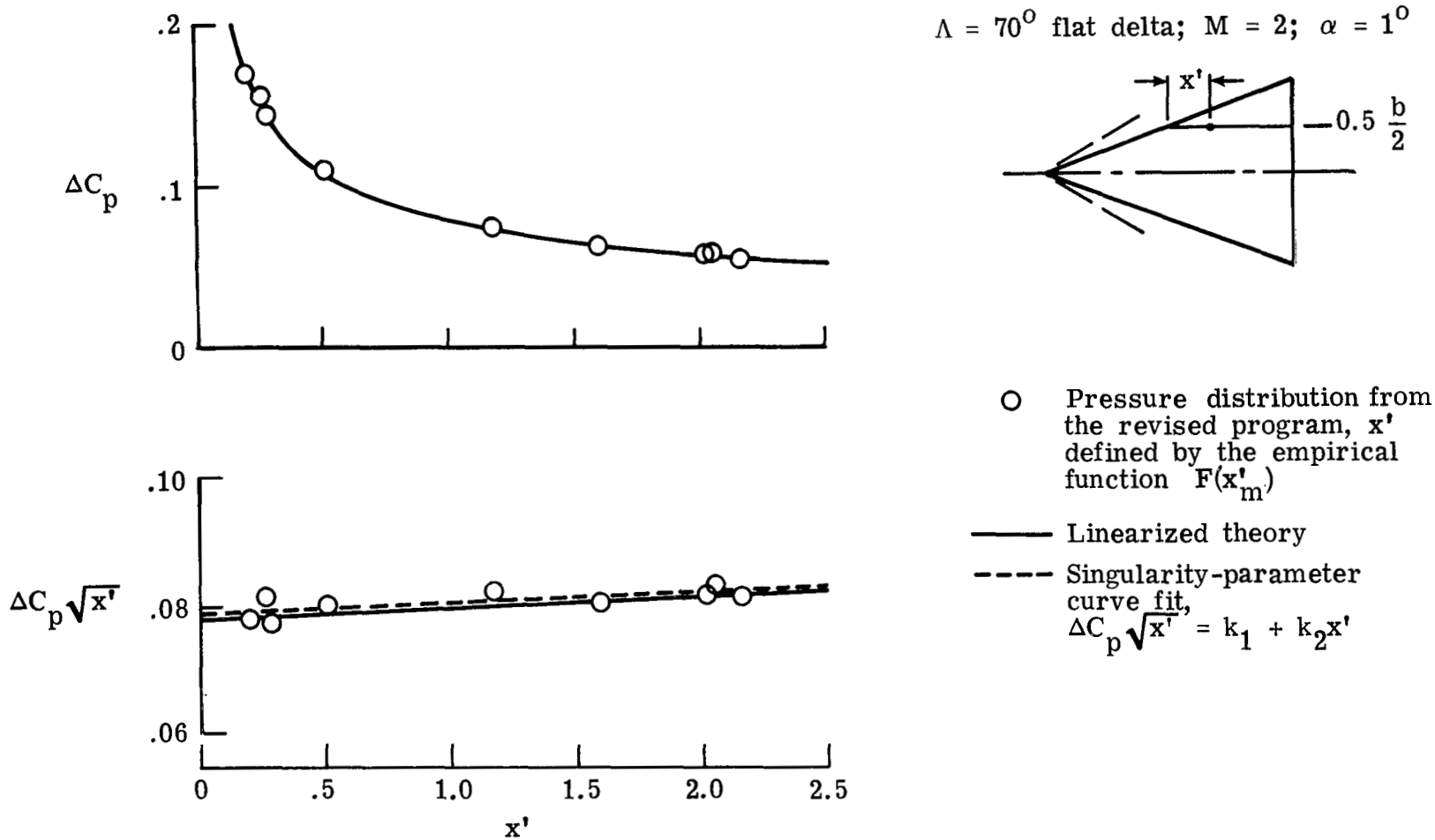

Figure 5.- An example of the application of a simple curve-fit function to adjusted data from the program of reference 8.

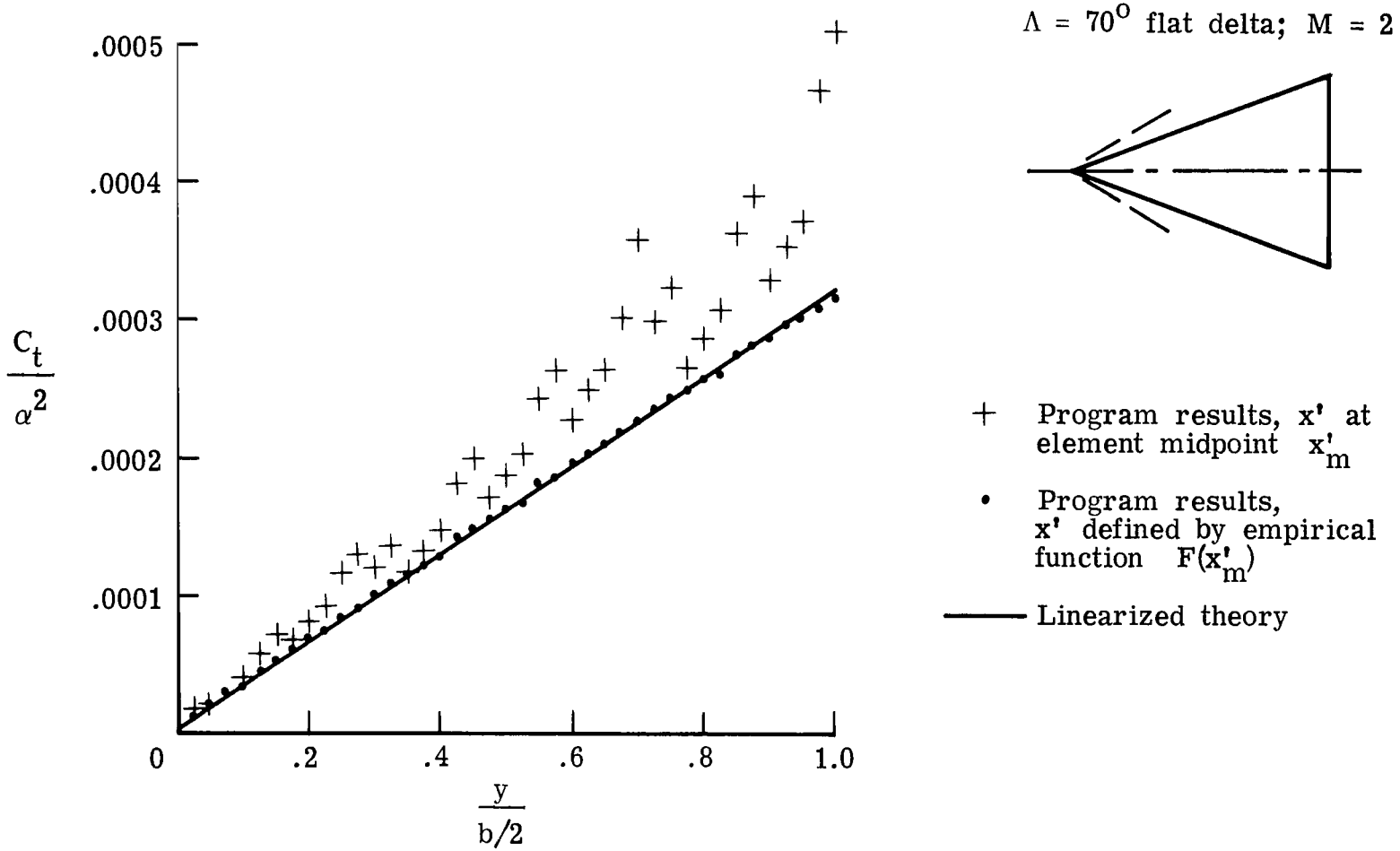

Figure 6.- Program thrust distribution with and without the empirical pressure-location adjustment.

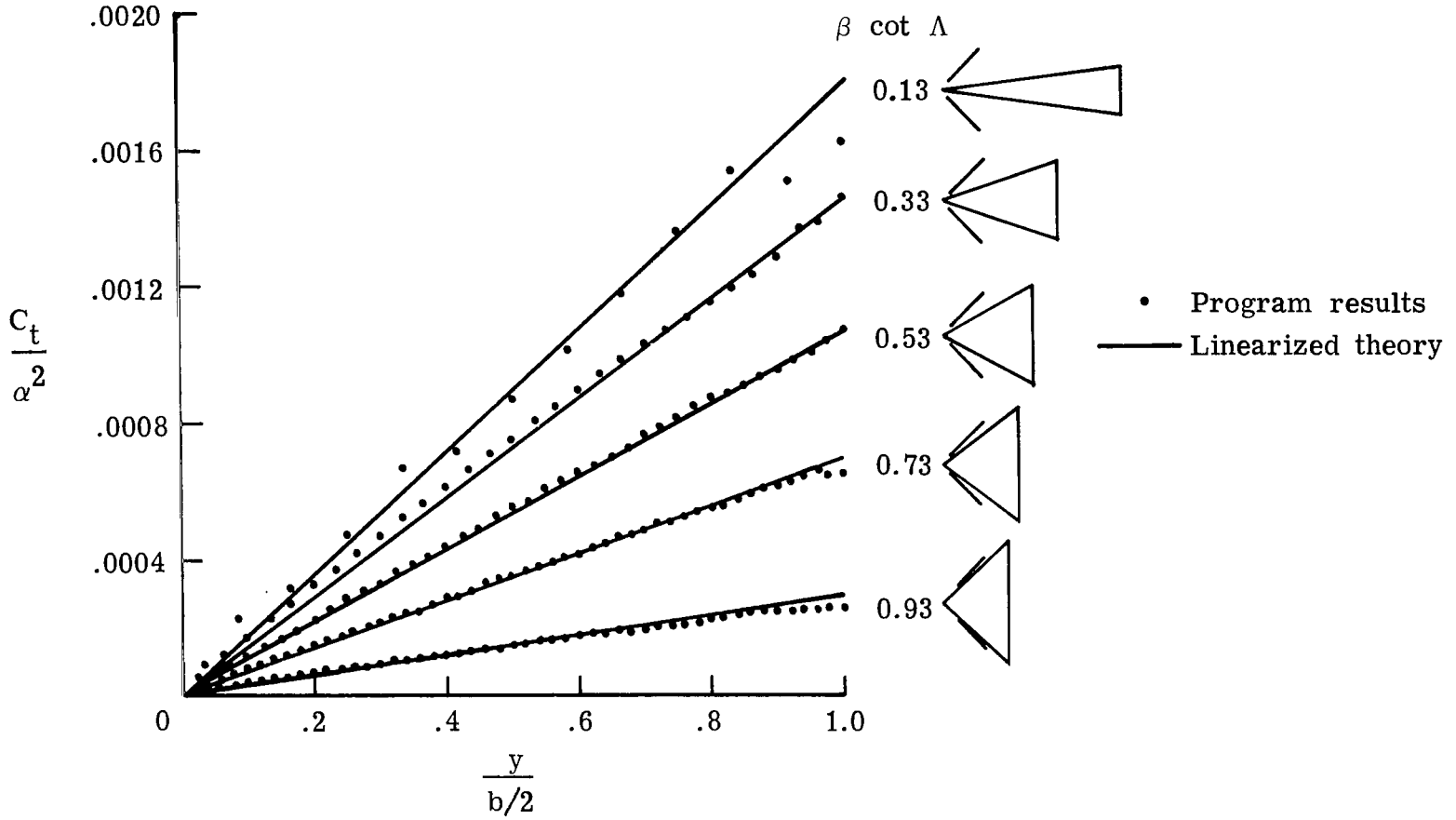

Figure 7.- Comparison of program and theoretical thrust distribution for flat delta wings covering a range of β cot Λ values.

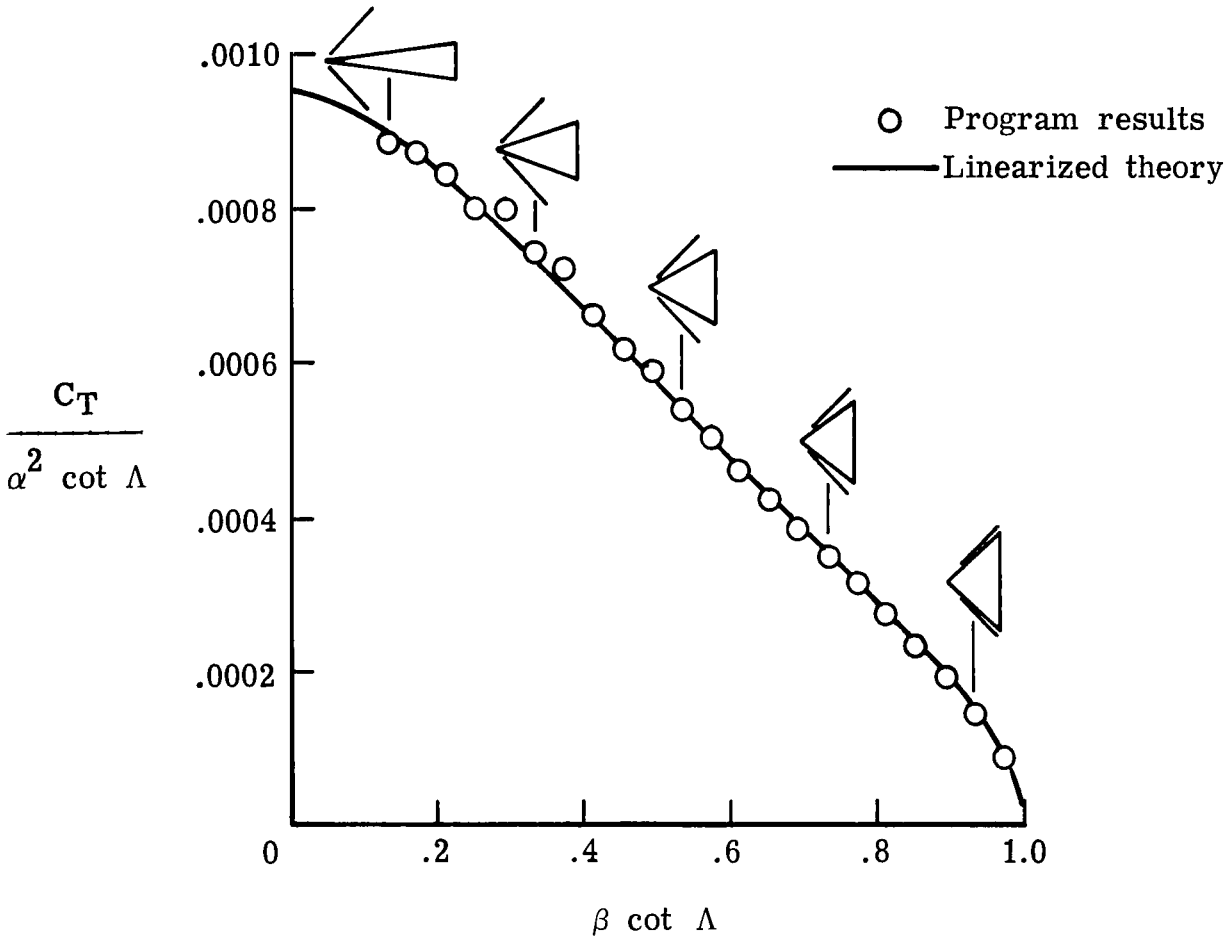

Figure 8.- Comparison of program and theoretical thrust coefficients for a series of flat delta wings.

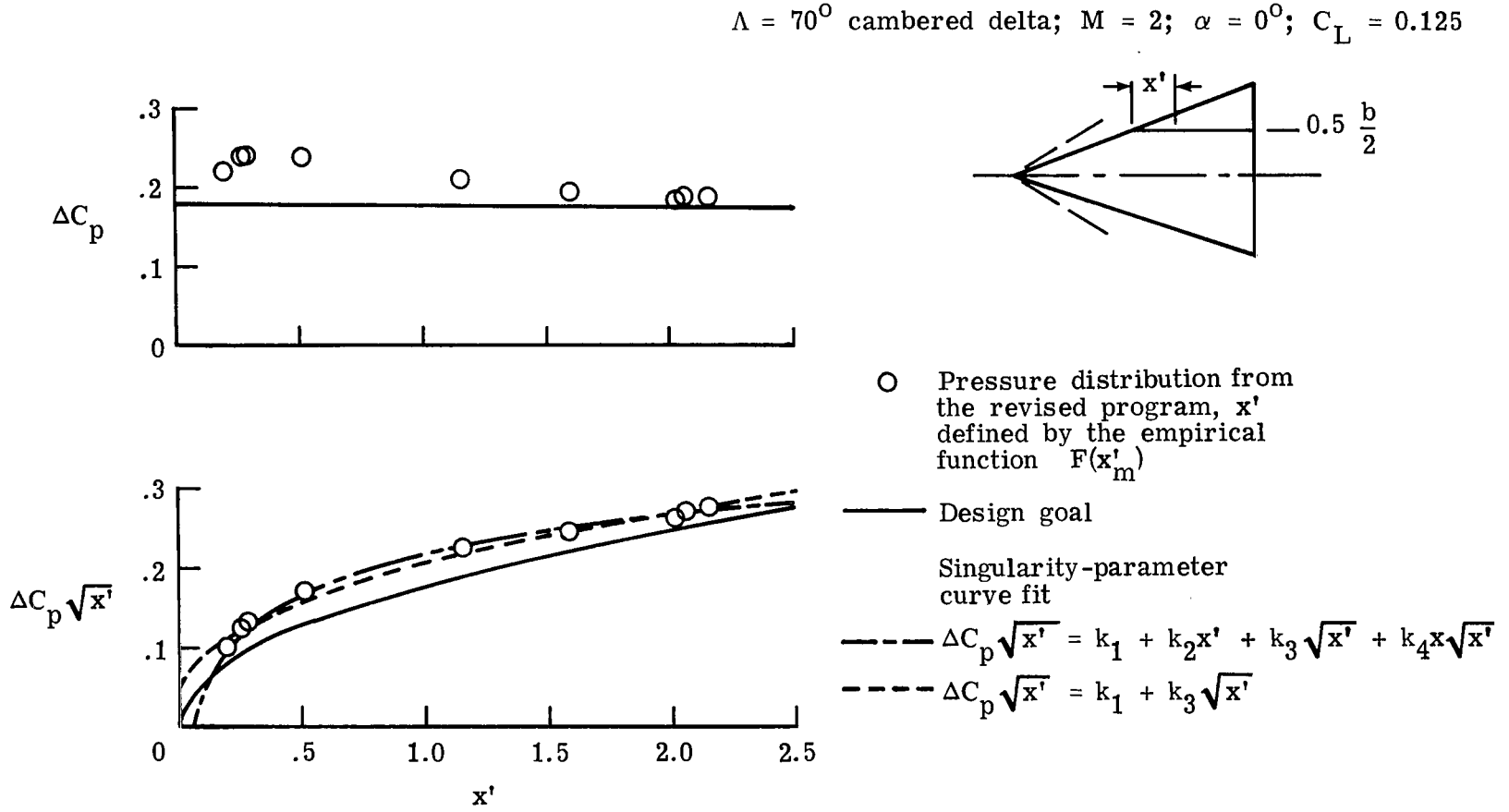

Figure 9.- An example of the application of simple curve-fit functions to adjusted data for a cambered wing at design lift condition.

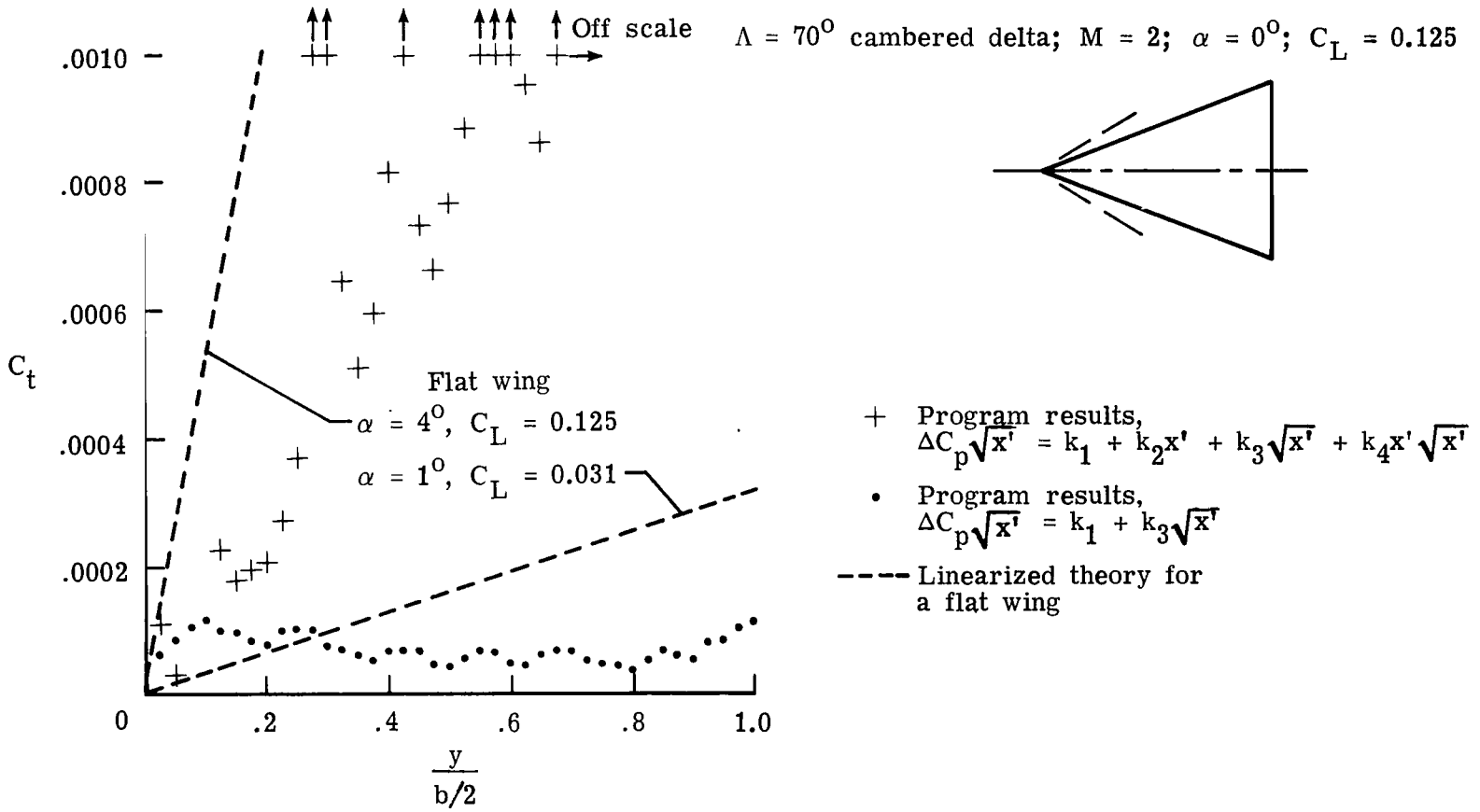

Figure 10.- Program thrust distribution for a cambered wing at design lift condition.

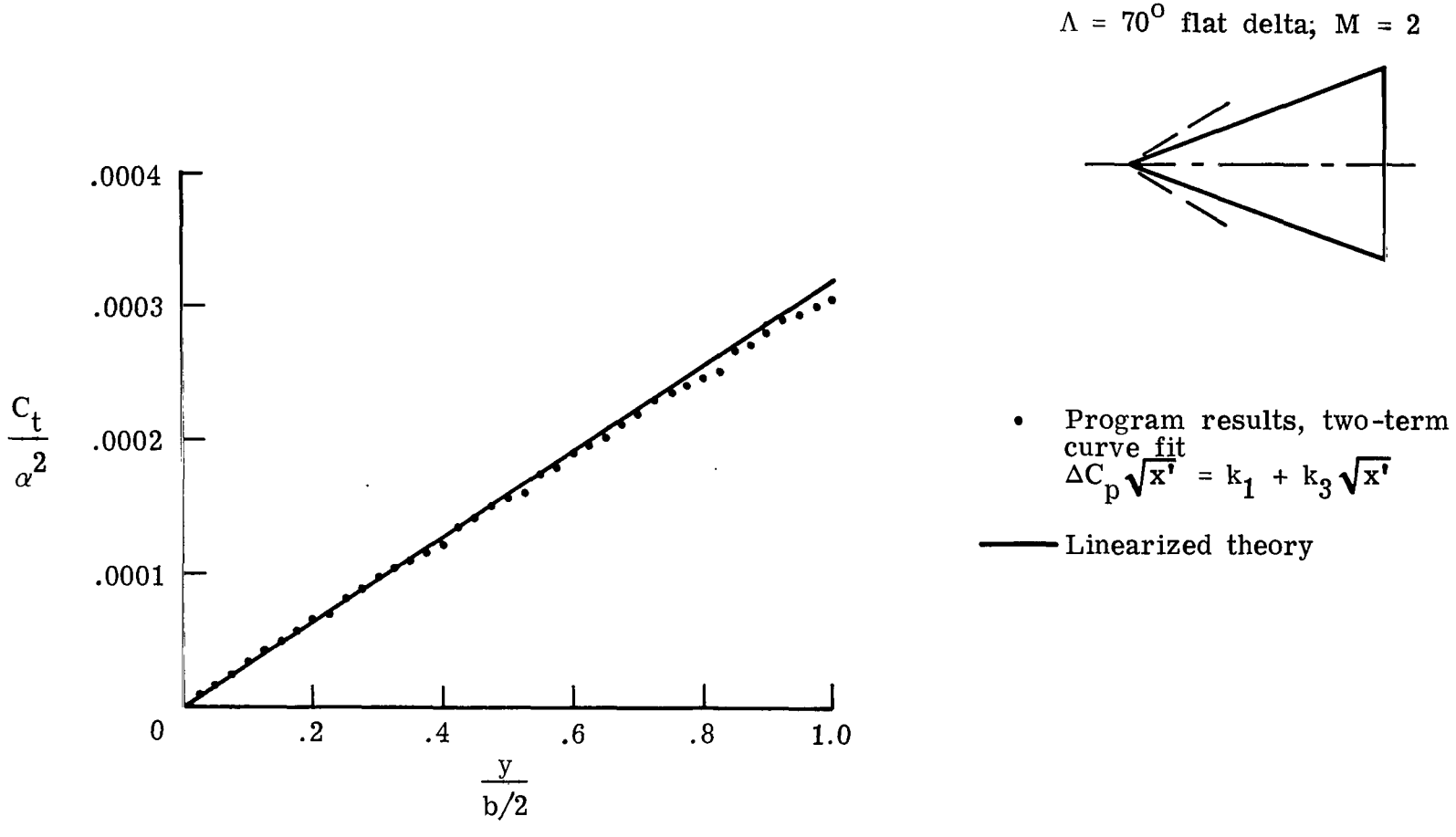

Figure 11.- Program thrust distribution for a flat wing treated as if it were a cambered wing.

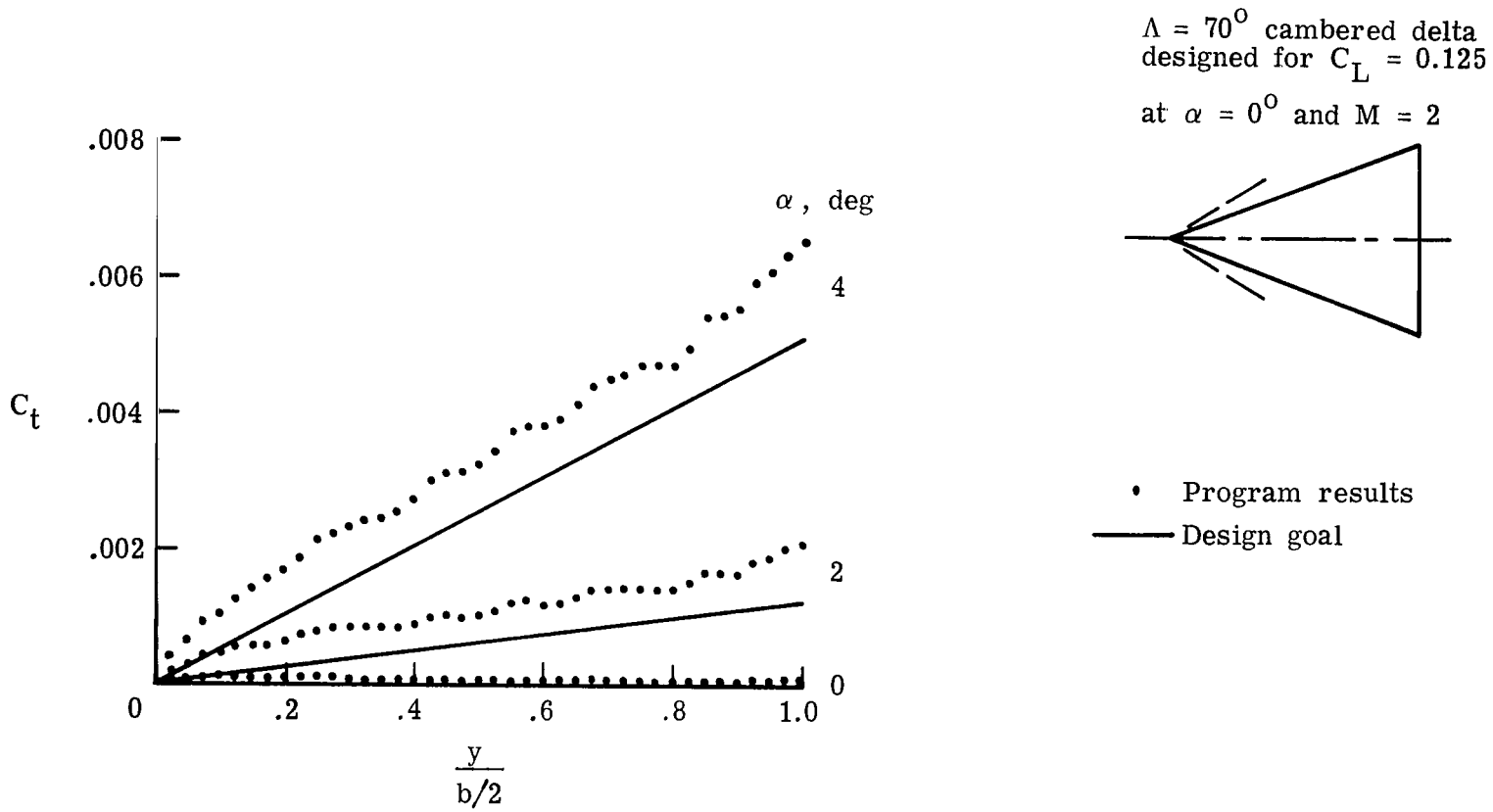

Figure 12.- Program thrust distribution for a cambered wing at several angles of attack.

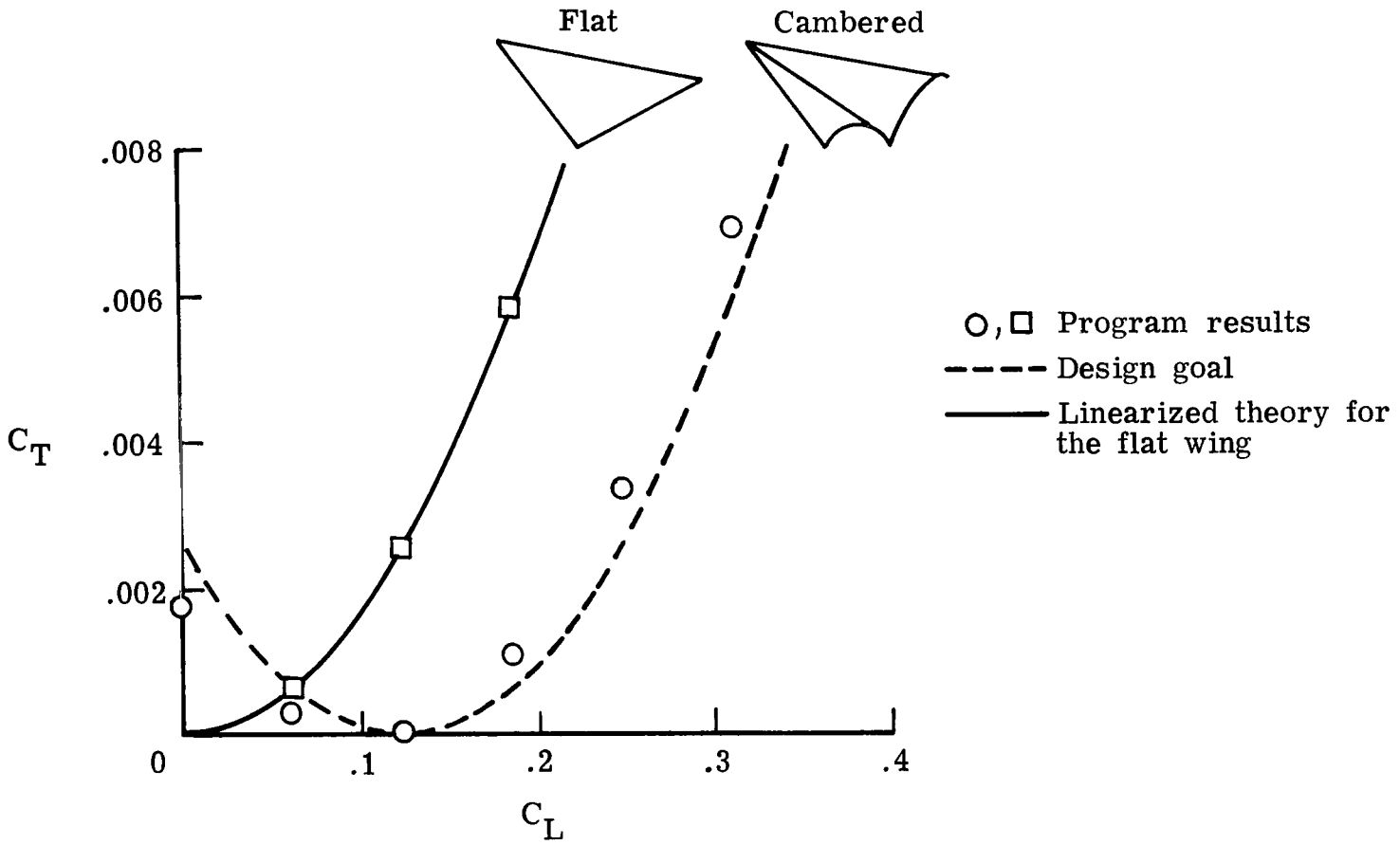

Figure 13.- Program thrust coefficient for a cambered wing and a comparison with data for a flat wing of the same planform. $\Lambda = 70^{\circ}$; $M = 2$.

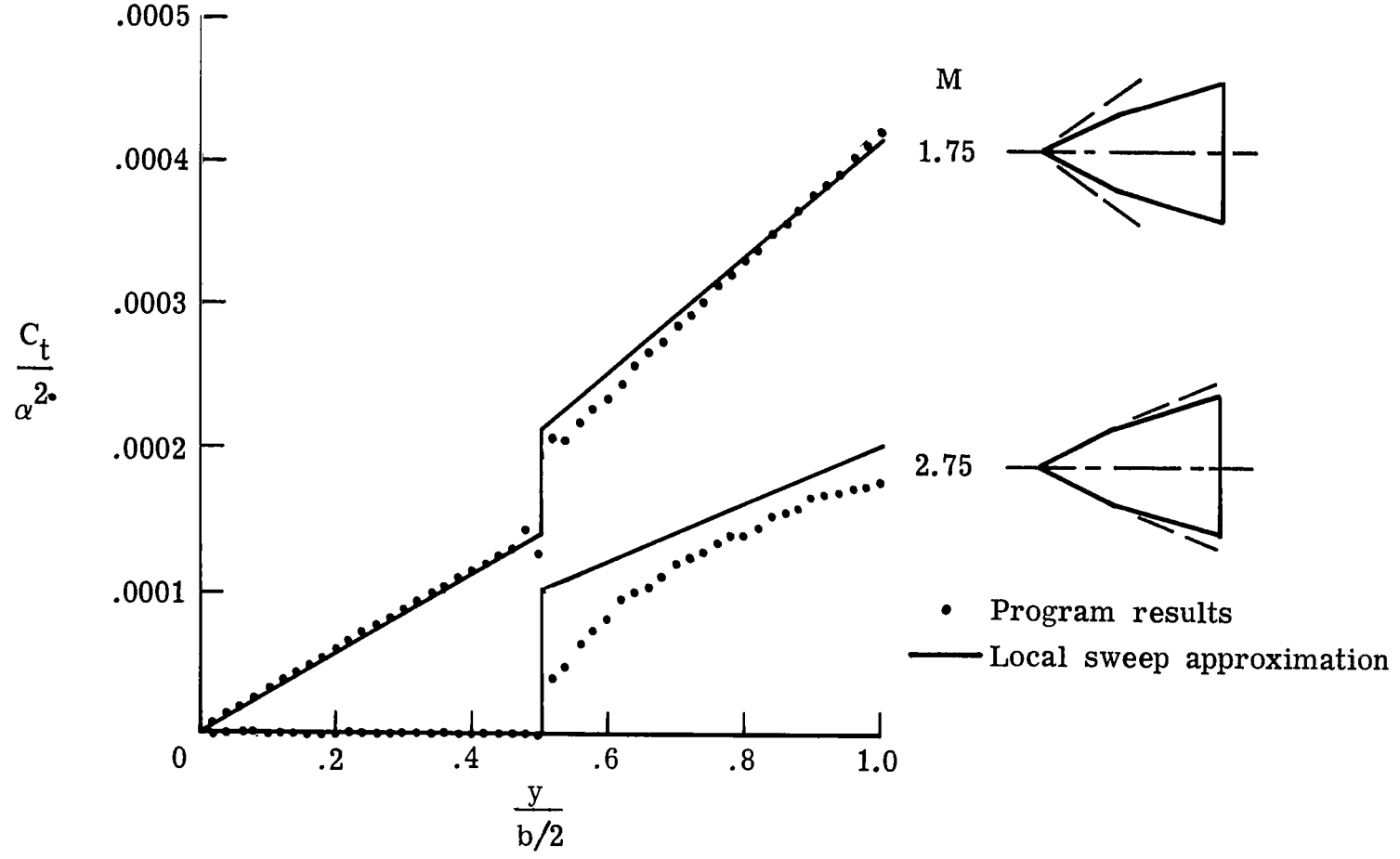

Figure 14.- Program thrust distribution for a cranked-leading-edge flat wing with a more highly swept outboard panel.

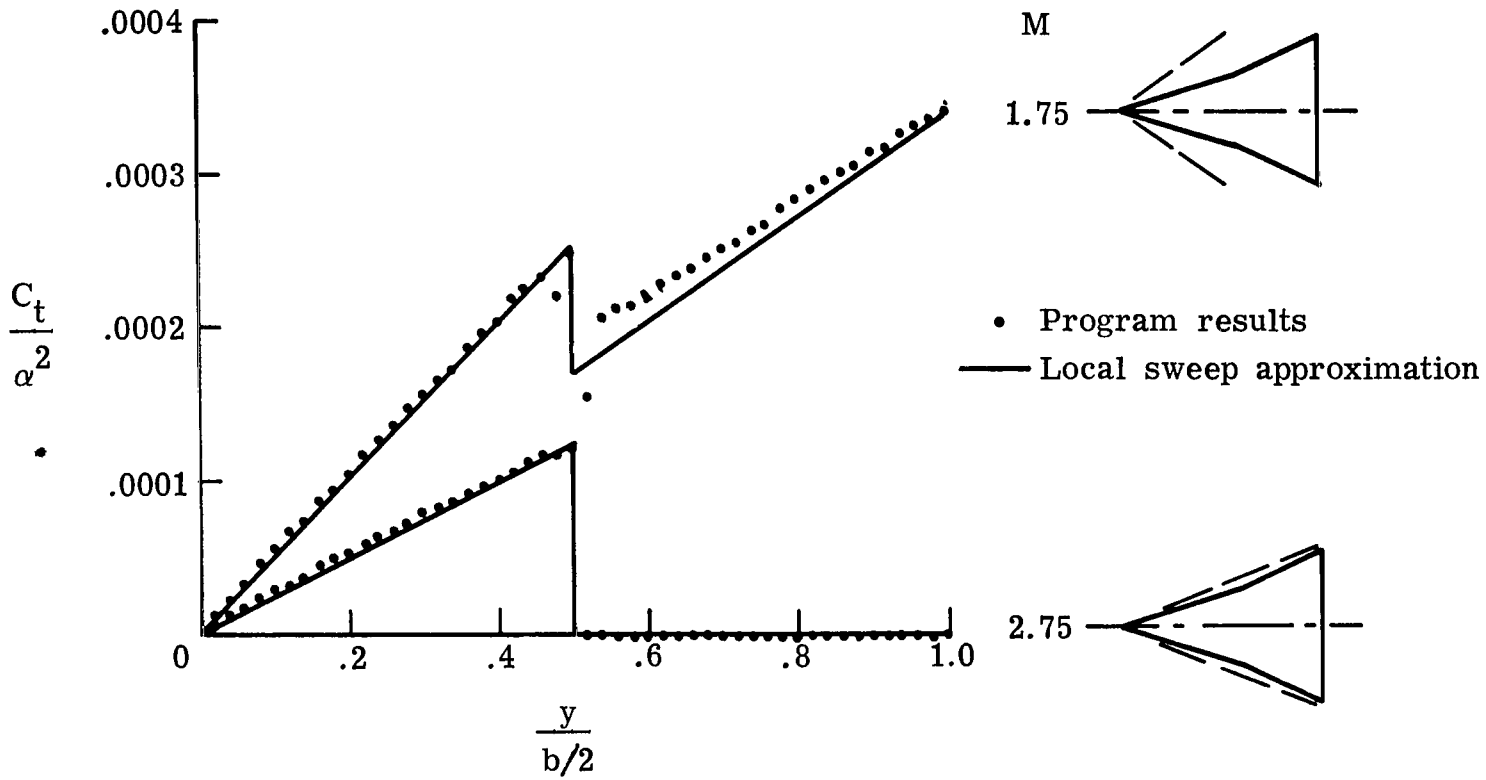

Figure 15.- Program thrust distribution for a cranked-leading-edge flat wing with a more highly swept inboard panel.

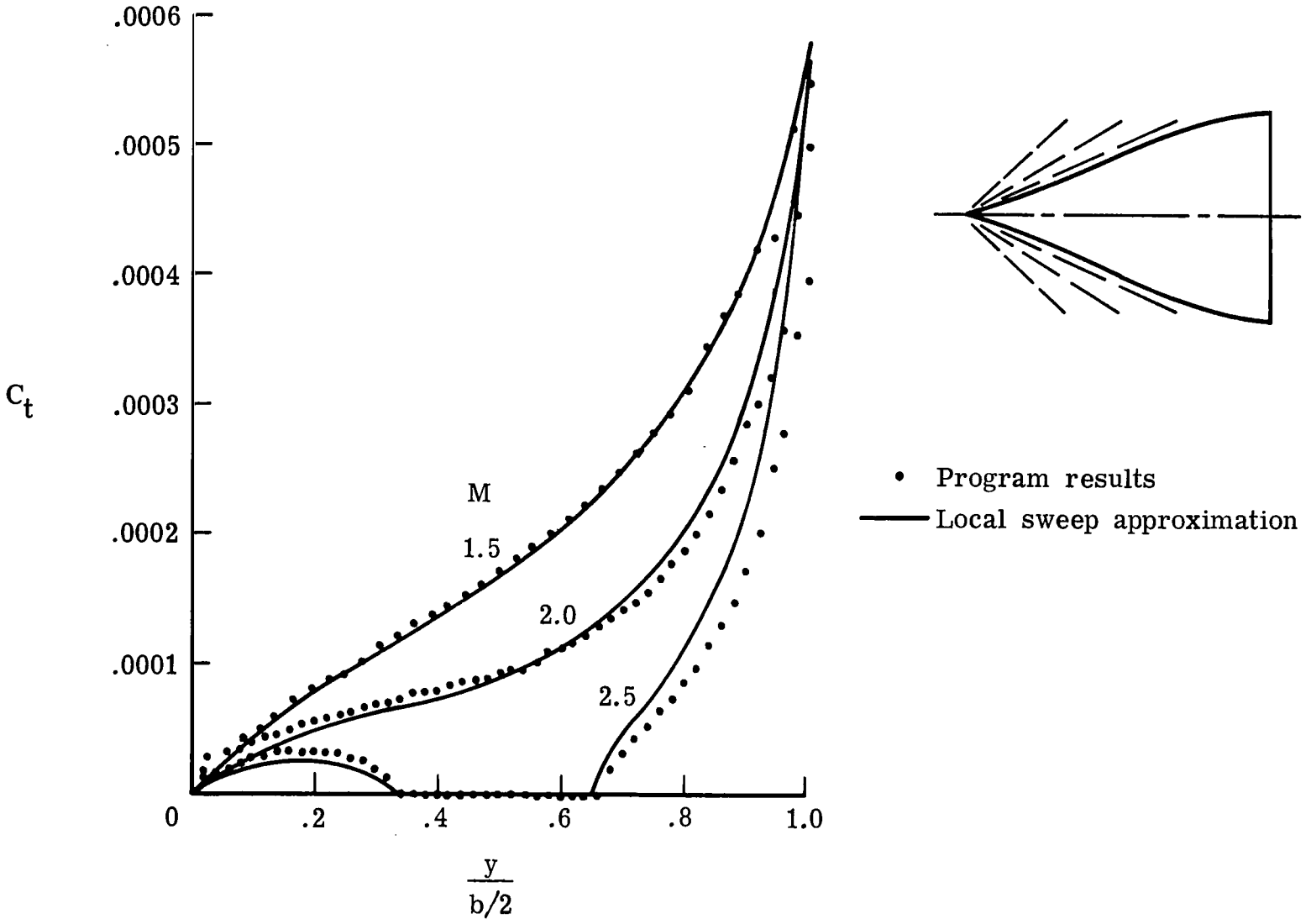

Figure 16.- Program thrust distribution for a flat "ogee" wing.

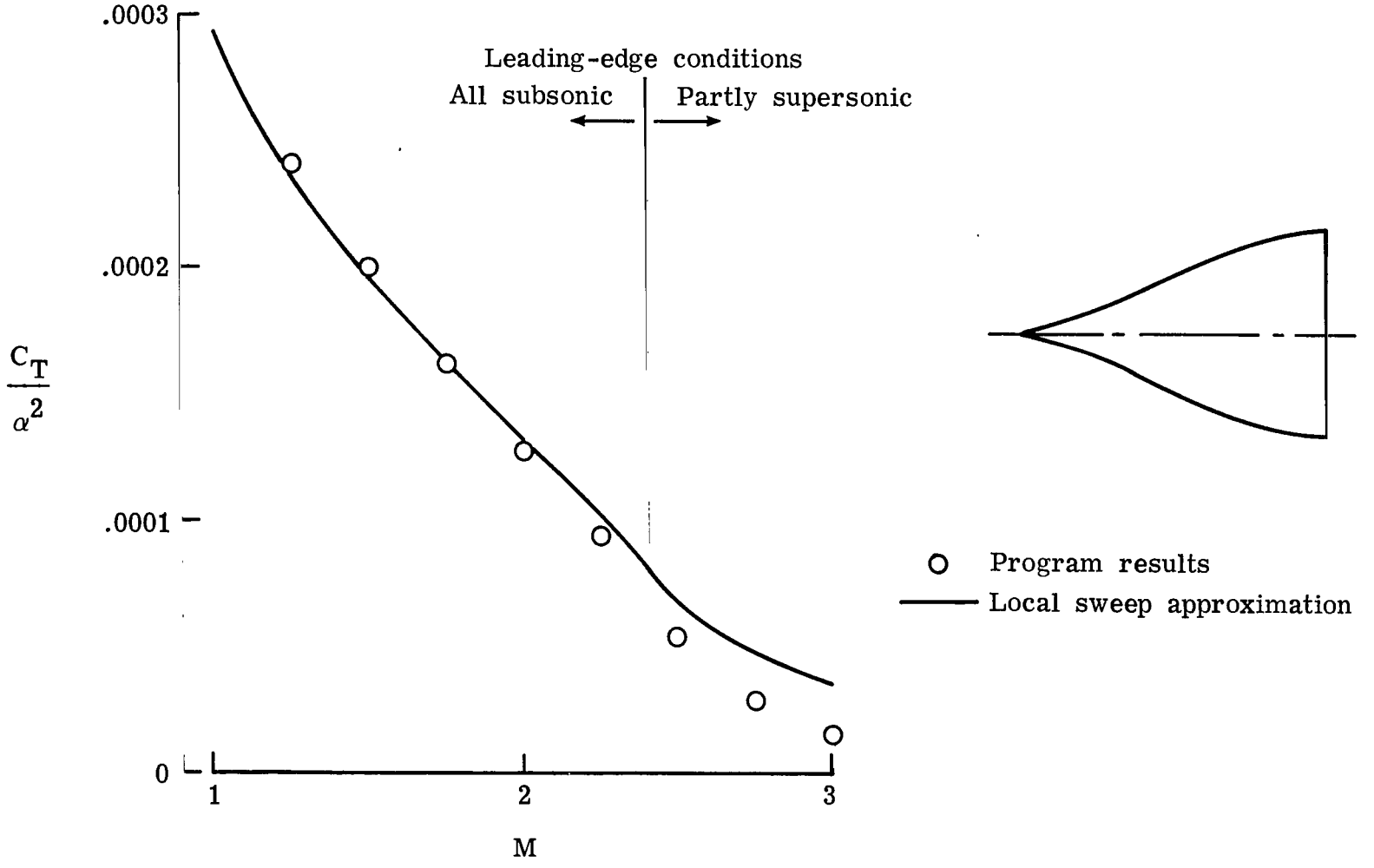

Figure 17.- Program thrust coefficients for a flat "ogee" wing.

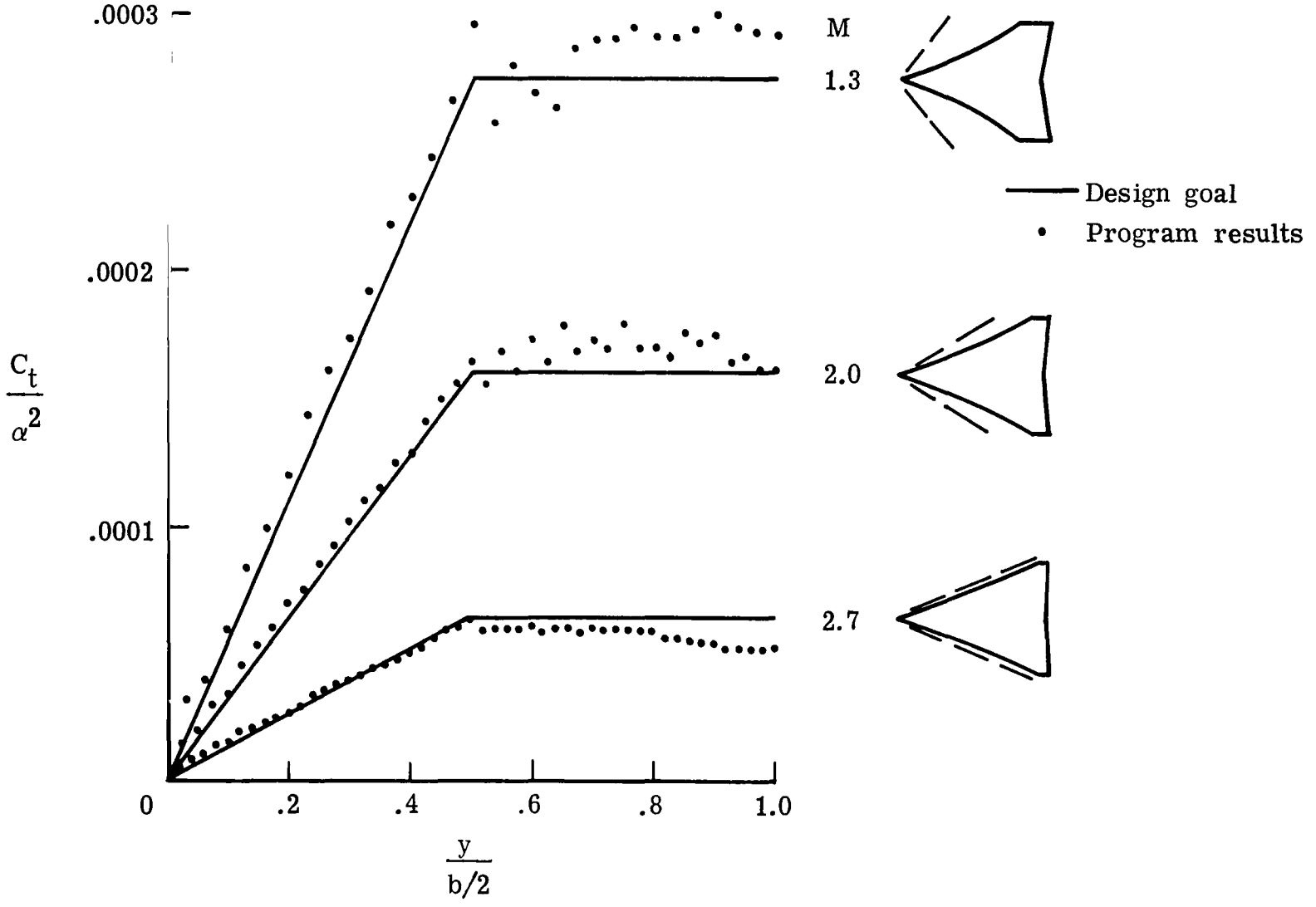

Figure 18.- Examples of wing planform design for specified thrust distribution.

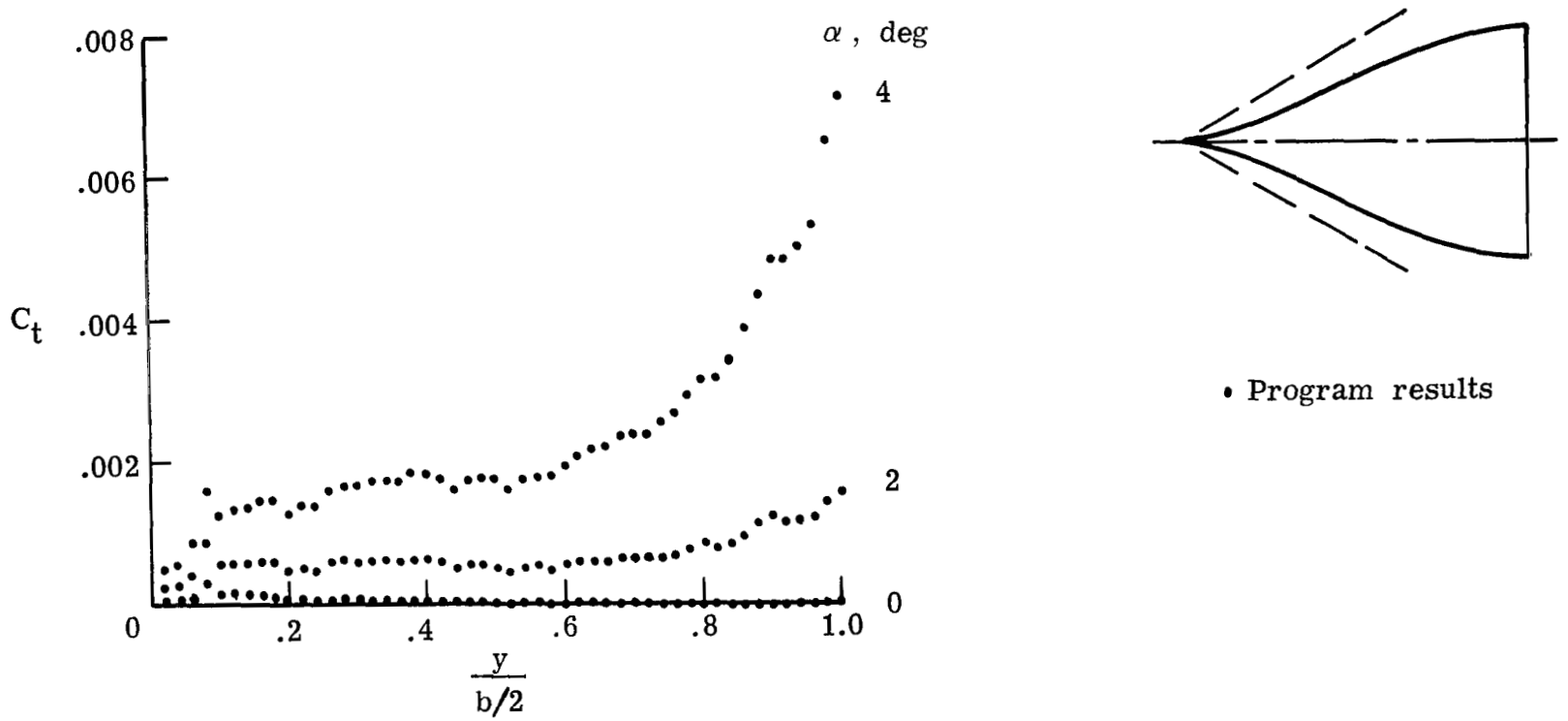

Figure 19.- Program thrust distribution for a cambered "ogee" wing at M = 2.

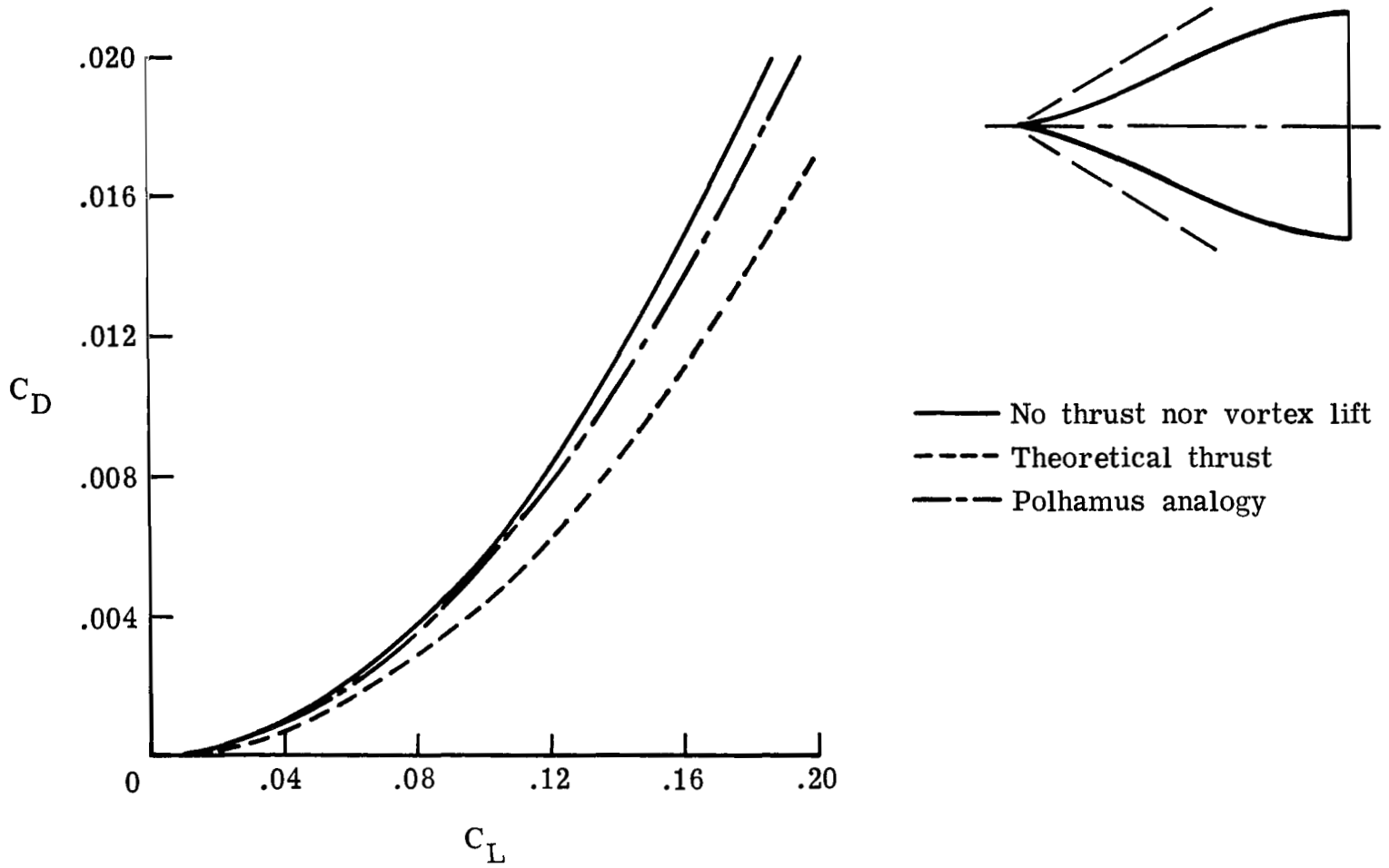

(a) Flat wing.

Figure 20.- Program lift-drag ratios for an "ogee" wing at M = 2.

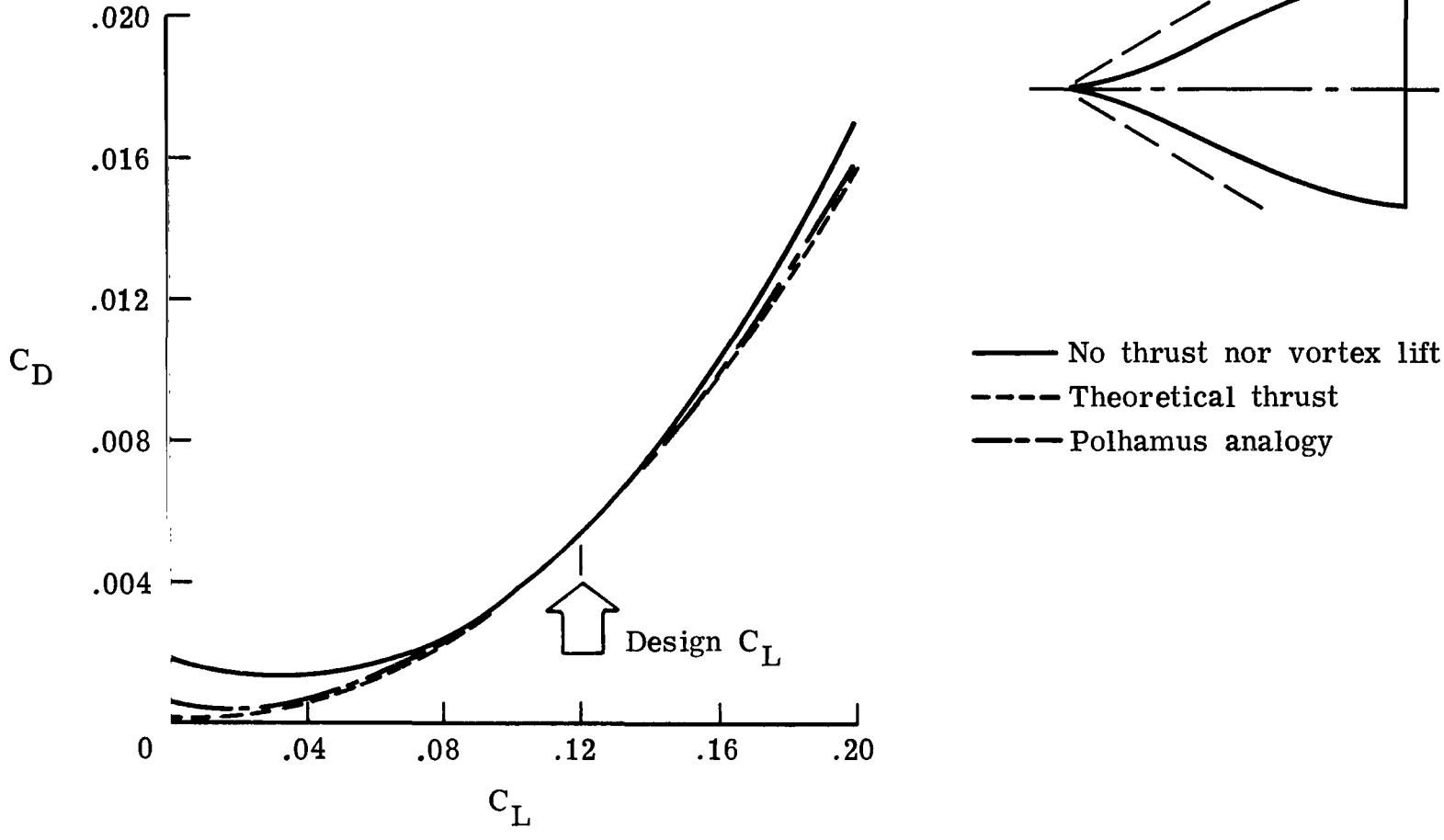

(b) Cambered wing.

Figure 20.- Concluded.

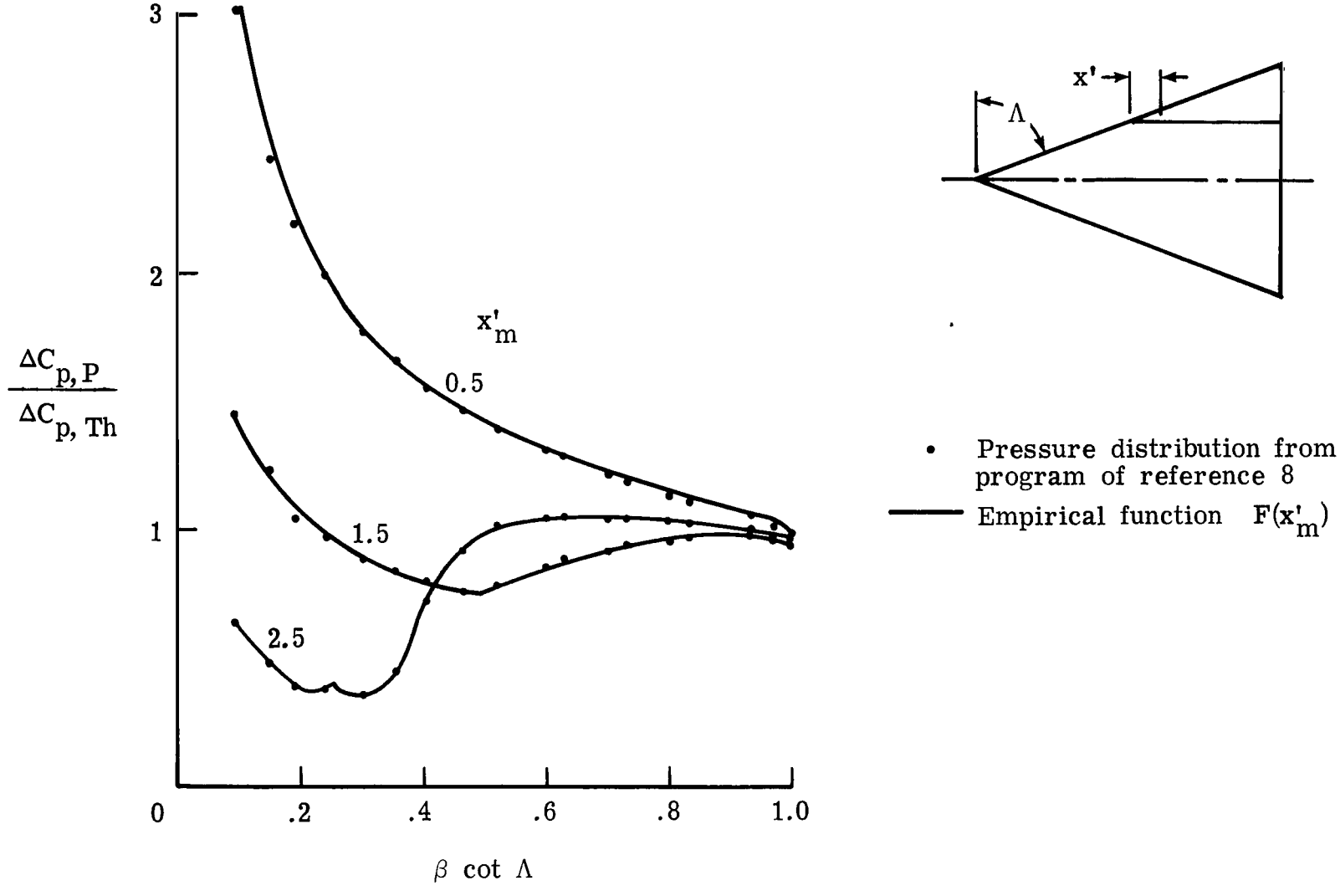

Figure 22.- Errors in the program of reference 8 as a function of β cot Λ for flat delta wings.

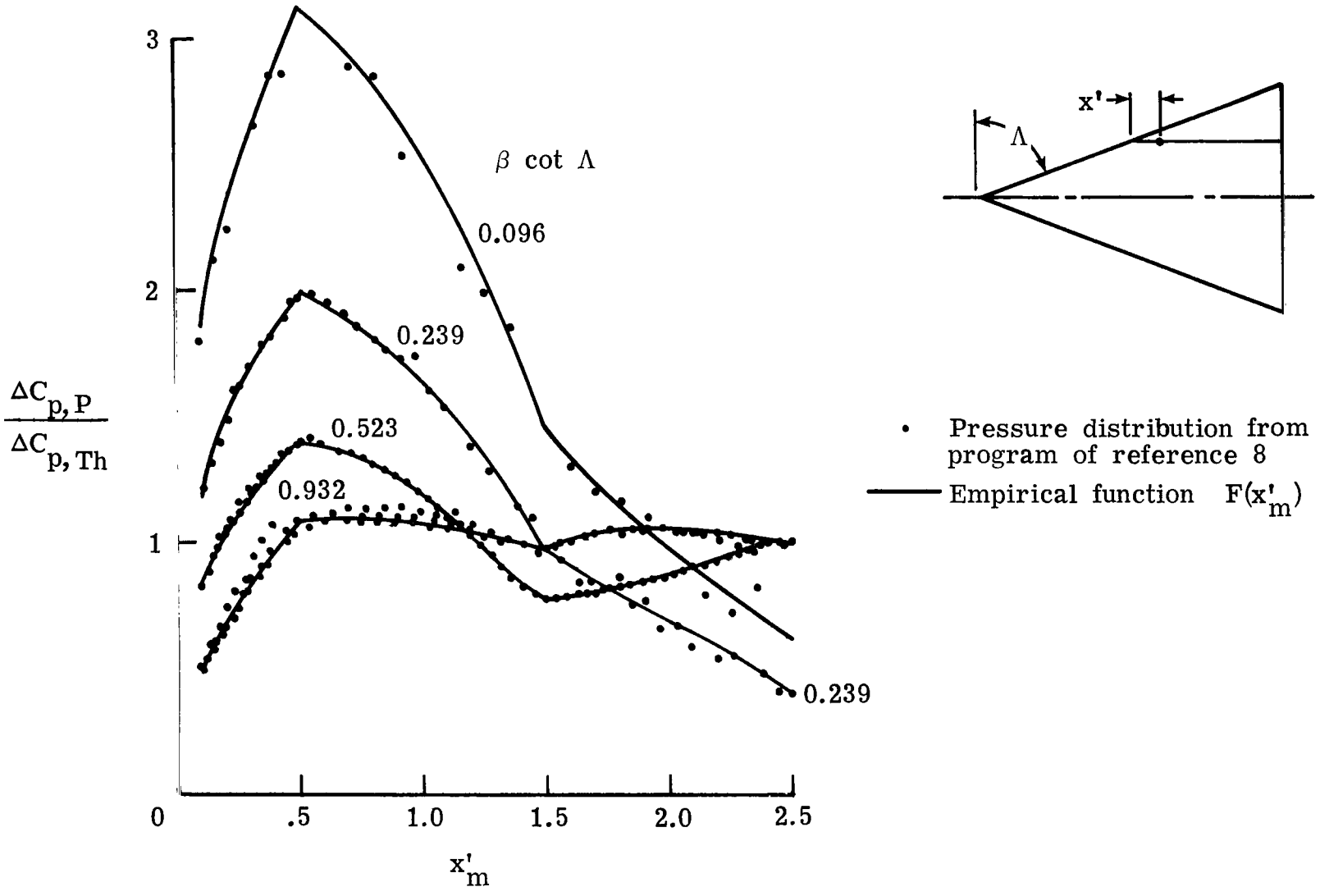

Figure 21.- Errors in the program of reference 8 as a function of x'_m for flat delta wings.

3 1 1U,A, 092978 S00903DS
DEPT OF THE AIR FORCE
AF WEAPONS LABORATORY
ATTN: TECHNICAL LIBRARY (SUL)
KIRTLAND AFB NM 87117